

SOME INNOVATIVE SURFACE TEXTURING TECHNIQUES FOR TRIBOLOGICAL PURPOSES

Journal:	<i>Part J: Journal of Engineering Tribology</i>
Manuscript ID:	JET-13-0251.R1
Manuscript Type:	Special Issue
Date Submitted by the Author:	n/a
Complete List of Authors:	Costa, Henara; Universidade Federal de Uberlandia, School of Mechanical Engineering Hutchings, I; University of Cambridge
Keywords:	surface texturing, lubrication, photochemical texturing, electrochemical texturing, inkjet printing
Abstract:	<p>This paper reviews methods for texturing surfaces for tribological applications, and presents some innovative methods that could make surface texturing more cost-effective. Possible texturing methods were identified and classified according to their physical principles. This involved identifying existing texturing methods and also led to proposals for new possible methods. Three innovative texturing methods with low cost and high texturing speed are then presented: i. a simpler and cheaper version of photochemical texturing; ii. maskless electrochemical texturing (MECT), and iii. masking surfaces by inkjet printing followed by etching. From these, MECT was the cheapest and fastest, but the minimum size of the texture features was the largest. Inkjet printing followed by etching is as an alternative that may potentially provide a good combination of cost and resolution, but the texturing time depends on the surface area. Then, an attempt was made to delimit tribological applications where the use of such processes could be beneficial, based on analysis of experimental results of their tribological evaluation. These showed that the methods proposed could be particularly suited for components with contact areas larger than the width of the texture features under either hydrodynamic lubrication or starved lubrication.</p>

SCHOLARONE™
Manuscripts

SOME INNOVATIVE SURFACE TEXTURING TECHNIQUES FOR TRIBOLOGICAL PURPOSES

Costa, H.L.¹ and Hutchings, I.M.²

¹ *Universidade Federal de Uberlândia, School of Mechanical Engineering ,
Laboratory of Tribology and Materials, Campus Santa Mônica, Sala IM220,
Uberlândia, MG, 38400901, Brazil, e-mail: ltm-henara@ufu.br, phone: +55
3432394036.*

² *University of Cambridge, Institute for Manufacturing, Dept. of Engineering, 17
Charles Babbage Road, Cambridge, CB3 0FS, UK, e-mail: imh2@cam.ac.uk, phone:
+44 1223765217.*

Abstract. This paper reviews methods for texturing surfaces for tribological applications, and presents some innovative methods that could make surface texturing more cost-effective. Possible texturing methods were identified and classified according to their physical principles. This involved identifying existing texturing methods and also led to proposals for new possible methods. Three innovative texturing methods with low cost and high texturing speed are then presented: *i.* a simpler and cheaper version of photochemical texturing; *ii.* maskless electrochemical texturing (MECT), and *iii.* masking surfaces by inkjet printing followed by etching. From these, MECT was the cheapest and fastest, but the minimum size of the texture features was the largest. Inkjet printing followed by etching is as an alternative that may potentially provide a good

1
2
3
4
5
6
7
8
9 combination of cost and resolution, but the texturing time depends on the surface area.
10 Then, an attempt was made to delimit tribological applications where the use of such
11 processes could be beneficial, based on analysis of experimental results of their
12 tribological evaluation. These showed that the methods proposed could be particularly
13 suited for components with contact areas larger than the width of the texture features
14 under either hydrodynamic lubrication or starved lubrication.
15
16
17
18
19
20

21
22 **Keywords:** *Surface texturing, inkjet printing, electrochemical texturing,*
23 *photochemical texturing hydrodynamic lubrication, starvation.*
24
25

26 **Nomenclature**

27
28
29 *a* - distance from the inlet to the first pocket

30
31 *B* - pocket width

32
33 *CW* - contact width

34
35 *d* - pocket diameter

36
37 *f* - fraction of area coverage

38
39 *h* – depth of the features

40
41 *l* – length of the arms of the chevrons

42
43 *p_x* – distance between features in the *x* direction

44
45 *p_y* – distance between features in the *y* direction

46
47 *t_o* – duration of intervals between working pulses

48
49 *t_p* – duration of working pulses
50
51
52
53
54
55
56
57
58
59
60

1
2
3
4
5
6
7
8
9 w – width of the lines

10
11 w_c - width of the arms of the chevrons

12
13 TS - non-dimensional parameter associated to the width of the pockets

14
15
16
17 *Greek symbols*

18
19
20 β – included angle of the chevrons

21
22
23 *Abbreviations*

24
25
26 3D – three-dimension

27
28 CFD - computational fluid dynamics

29
30 CNC – computer numerical control

31
32 CVD – chemical vapour deposition

33
34 EBT – electron beam texturing

35
36 ECP - electrochemical printing

37
38 EDM - electro discharge machining

39
40 EDT - electro discharge texturing

41
42 EHL - elastohydrodynamic lubrication

43
44 FEM – finite element modelling

45
46 FIB – focused ion beam

47
48
49 HAB - hot air blower

1
2
3
4
5
6
7
8 IBT – ion beam texturing

9
10 IMS = industrial methylated spirit

11
12 LT – laser texturing

13
14 MECT - maskless electrochemical texturing

15
16 PCT - Photochemical texturing

17
18 SEM – scanning electron microscopy

19
20 USC – ultrasonic cleaning

21
22 UV – ultra violet
23
24
25
26
27
28

29 30 **1. Introduction**

31
32 Surface texturing consists of modifying surface topography in order to create a
33
34 uniform microrelief composed of regularly distributed asperities or depressions with
35
36 controlled geometry. Surface texturing has been used for many different purposes [1],
37
38 including improvement of tribological performance. The mechanisms responsible for
39
40 improving the tribological performance of textured surfaces can vary significantly
41
42 between applications and positive results have been shown for situations varying from
43
44 dry sliding [2], to solid lubrication [3], hydrodynamic lubrication [4-10],
45
46 elastohydrodynamic lubrication (EHL) [11, 12] and mixed lubrication [13, 14]. In
47
48 addition, surface texturing can help to entrap wear debris [15]. However, the successful
49
50 use of surface texturing in tribological applications still faces two main challenges: *i.*
51
52
53
54
55
56
57
58
59
60

1
2
3
4
5
6
7
8
9 careful design of the texture patterns is necessary for surface texturing to be beneficial,
10 and *ii.*: cost-effective surface texturing methods need to be designed for situations
11 involving large volume production of cheap components.
12
13

14
15 One of the most successful tribological applications of surface texturing is the
16 increase of load bearing capacity of moving surfaces under hydrodynamic lubrication.
17 Considerable effort in the last two decades has tried to optimize the increase of load
18 bearing capacity and the reduction of friction in hydrodynamic lubrication as a function
19 of either texture parameters, such as shape, size and distribution of the features that
20 compose the pattern, or operational parameters, such as load and speed [5-7]. Particular
21 emphasis should be given to the extensive work carried out by Etsion and collaborators.
22 They have developed analytical models to solve the Reynolds equation for textured
23 surfaces for different engineering applications and a good review of their work can be
24 found in [8]. More recently, other researchers have suggested that the use of mass-
25 conserving algorithms to solve the Reynolds equation numerically might be more
26 adequate for cavitated films [16, 17], since the occurrence of cavitation is responsible
27 for the asymmetrical pressure distribution over individual pockets and therefore a net
28 load support for textured surfaces. Fowell et al. [16] argue that mass-conserving
29 algorithms can provide more realistic accounts of the benefits achievable when
30 texturing hydrodynamic bearings. Another, different approach has used CFD
31 simulations, based on the numerical solution of the Navier–Stokes and energy equations
32
33
34
35
36
37
38
39
40
41
42
43
44
45
46
47
48
49
50
51
52
53
54
55
56
57
58
59
60

1
2
3
4
5
6
7
8
9 for incompressible flows [9]. Experimental work has also showed the benefits of surface
10 texturing under hydrodynamic lubrication [4, 8, 10, 18]. Some common points emerge
11 from the works cited above, independently of whether they use theoretical or
12 experimental approaches. In particular: *i*, preferably, the contact should be only
13 partially textured, which limits the width of the individual features, so that in general
14 positive results have been shown mostly for feature widths within the range of 10-100
15 μm ; *ii*, the ratio between the depth and the width of the features should be small,
16 generally in the range from 0.05 to 0.15. This limits the depth of the features, so that
17 normally, good results have been reported for feature depths in the range from around 1
18 to 15 μm .

19
20
21
22
23
24
25
26
27
28
29
30
31 The case of EHL is more challenging, but some researchers have also shown good
32 results if the width of the micro features is substantially smaller than the contact width.
33 Observation of the contact area by optical interferometry has shown that the lubricant
34 expelled from the micro features can help to separate rubbing surfaces, especially under
35 thin film lubrication conditions [11]. Experimental and numerical investigation of one
36 individual micro feature (a circular dimple) inside an EHL contact under rolling-sliding
37 conditions showed that deep dimples induced failure of the oil film, but shallow dimples
38 generated a large increase in film thickness [12]. These authors believe that shallow
39 features maintain the viscosity of the lubricant inside them high enough so that shearing
40 can expel it to locally enhance film thickness. Due to the small size of EHL contacts, the
41
42
43
44
45
46
47
48
49
50
51
52
53
54
55
56
57
58
59
60

1
2
3
4
5
6
7
8
9 width of the micro features that compose the texture generally becomes limited to
10 values below 100 μm , and, according to the results of Mourier et al. [12], the depth
11 should be preferably below 1 μm .
12
13

14
15 All the results described above for the effects of surface texturing on lubrication were
16 obtained for contacts fully immersed in lubricant, i.e. there is always enough lubricant
17 to fill the contact inlet. However, if lubricant starvation occurs in the contact, the film
18 thickness will also depend on the amount of lubricant available in the contact [19].
19
20 Although lubricant side flow reduces film thickness in a starved contact when compared
21 with an immersed contact, this lubricant may flow back to the contact inlet in the
22 process known as lubricant replenishment [20, 21]. In such situations, the texture
23 features can be expected to act as lubricant micro-reservoirs that help to replenish the
24 contact inlet, but it seems that no theoretical modeling yet exists to investigate this
25 effect. The effect of surface texturing on friction under starved lubrication was
26 investigated for polyoxymethylene [22], and it was observed that for very large aspect
27 ratio between the depth and width of the micro features the lubricant “disappeared”
28 from the contact and no friction reduction was detected. A similar lack of benefit from
29 textured surfaces was found in [18] when very deep features were used under starved
30 lubrication conditions.
31
32
33
34
35
36
37
38
39
40
41
42
43
44
45
46
47

48 The most successful method used today to texture surfaces in engineering
49 applications is laser texturing [8]. It has been used to texture a wide range of materials,
50
51
52
53
54
55
56
57
58
59
60

1
2
3
4
5
6
7
8
9 from polymers [23] to metals [8, 24] and ceramics [15, 25]. Also, it allows the
10 production of patterns with small features. For examples, feature depths of 200 nm and
11 diameters of 20 μm could be obtained in steel samples by using a femtosecond pulse
12 laser [12]. The use of more sophisticated optics can lead to beam sizes below 5 μm .
13 Another approach, based on laser-induced periodic surface structuring, used a
14 femtosecond laser to produce an array of dimples with diameters of 1 μm , although the
15 array of the dimples was not deterministic [26]. However, the use of laser texturing
16 presents limitations. First, the ablation mechanism often leads to the formation of raised
17 features around the pockets, which originate from the ejected molten material. These
18 lateral rims are normally hard due to the microstructural changes caused by the process
19 and can cause severe abrasive wear of the countersurface. After texturing, they
20 therefore need to be removed, either by mechanical polishing, or by laser polishing [27,
21 28]. This phenomenon is practically eliminated when very short pulses (e.g. from
22 femtosecond lasers) are used.

23
24
25
26
27
28
29
30
31
32
33
34
35
36
37
38
39
40
41
42
43
44
45
46
47
48
49
50
51
52
53
54
55
56
57
58
59
60
The second issue for laser texturing is the texturing speed. The process involves
ablation, which changes the material state directly from solid to vapour in very short
period of time, with little metallurgical surface damage. The ablation fluence threshold
for materials varying from soft metals to glasses and hard composites stays in the range
from 0.2 to 20 J cm^{-2} [29]. If the laser system has a sufficiently high maximum pulse
energy, a micro dimple can be produced through laser ablation using a stationary laser

1
2
3
4
5
6
7
8
9 spot with a size comparable to the dimple, and without the need for laser spot scanning,
10
11 as long as the laser fluence (pulse energy/laser spot area) can at least exceed the ablation
12
13 threshold fluence for the target material [28], and then the depth of the dimple will
14
15 depend on the number of pulses. The use of high pulse energies, small spot diameters
16
17 and (ultra)short pulse durations has allowed material removal by ablation to be achieved
18
19 for a wide range of materials at increasing texturing speeds. However, since the features
20
21 are normally produced in a serial sequence, the texturing time for larger components can
22
23 still be long, in particular for cheaper laser texturing facilities, that use long pulse
24
25 durations and large spot sizes. Many components that could have their performance
26
27 increased by surface texturing are normally cheap, so they might require cheaper
28
29 texturing methods in order for the increase in tribological performance achieved through
30
31 texturing to be cost-effective. An alternative laser texturing technique that is
32
33 substantially faster is laser interference texturing [30]. In this technique, interference
34
35 fields produced by several coherent high power laser beams can produce periodic
36
37 patterns composed of line-nets or dot-like features. The interference pattern covers a
38
39 size corresponding to the beam diameter, which increases texturing speed substantially,
40
41 but the maximum sizes of the individual features can be too small for some lubricated
42
43 tribological applications (up to around 3 μm in width and 1 μm in depth). Therefore,
44
45 such features might be desirable for applications involving EHL, but too small for
46
47 hydrodynamic lubrication or starved lubrication. Another possible problem is that the
48
49
50
51
52
53
54
55
56
57
58
59
60

1
2
3
4
5
6
7
8
9 process changes the topography of the whole surface, instead of only creating localized
10 ablated features.

11
12
13 Other texturing methods have also been reported in the literature. Major advances in
14 microfabrication have driven the area of surface texturing. In principle, many of the
15 methods used in the microelectronics industry might be adapted to surface texturing.
16
17 This paper reviews innovative texturing methods proposed and investigated by the
18 present authors in recent years.
19
20
21
22
23

24 The aim was to explore some innovative surface texturing methods, to allow the
25 benefits of surface texturing to be better explored in a wider range of practical
26 applications, and to discuss their applicability to improve tribological performance. The
27 next section presents a survey of possible texturing methods, classified according to the
28 physical processes by which a surface texture could be produced. Conventional
29 manufacturing methods that employ these physical principles have been studied. In
30 addition, some new possible texturing methods that fall within the same groups have
31 been proposed. After listing all possible texturing methods, an attempt is made to
32 classify and compare them. Three methods that emerged from this comparison have
33 been explored experimentally and their advantages and limitations are summarized. The
34 criteria involved in selecting these methods were one or more of the following:
35 simplicity of the technique, low cost, high texturing speed, and flexibility in terms of
36 pattern geometry. Finally, the paper attempts to delimit tribological applications where
37
38
39
40
41
42
43
44
45
46
47
48
49
50
51
52
53
54
55
56
57
58
59
60

1
2
3
4
5
6
7
8
9 their use could be beneficial, by examining experimental results from their tribological
10 evaluation.
11

12 13 14 **2. Survey of possible surface texturing methods** 15

16 Alternative manufacturing technologies for surface texturing are needed to
17 overcome the challenges of volume production. The technologies should be cheap and
18 flexible, both in terms of the shapes of the features to be produced and the shapes of the
19 surfaces to be textured. This section identifies most of the existing texturing methods
20 and also proposes some new possible methods. However, the review is non-exhaustive
21 because surface texturing has been extensively studied in recent years and new
22 techniques appear very quickly. The methods have been categorized into four main
23 groups according to their physical principles:
24
25
26
27
28
29
30
31
32

33
34 **Adding material:** the pattern features are created by addition of material to the
35 desired surface, creating small areas of relief [31-47].
36
37

38 **Removing material:** the features are created by removal of material of the surface,
39 creating small depressions [4, 8, 12, 15, 23-25, 48-75].
40
41

42 **Moving material:** the change in the surface structure is attributable to plastic
43 deformation and redistribution of material from some parts of the surface to others [14,
44 30, 48, 76-81].
45
46
47
48
49
50
51
52
53
54
55
56
57
58
59
60

1
2
3
4
5
6
7
8
9 **Self-forming:** wear-resistant regions are formed on a surface, so that a texture
10 develops through wear of the surface, with the wear-resistant regions being left standing
11 above the surrounding material [82-85].
12
13

14
15 Tree structures for each family with their taxonomy are presented in Figure 1 and
16 references are presented for individual processes if possible. All the processes marked
17 by ‘*’ are processes that require a masking step before the texturing step. In Figure 2,
18 methods that could be used to mask the surfaces are organized in a tree structure [86-
19 95].
20
21
22
23
24
25

26 In view of the wide variety of possible methods available for texturing surfaces, the
27 choice for a specific method becomes difficult. Normally, the selection procedure is
28 task-based and starts with the definition of requirements of a certain application. Most
29 of the texturing methods screened are new and not yet well studied, which complicates
30 the selection further. In order to assist this task, a database of texturing methods was
31 created using CES Constructor (Granta Materials) of which details can be found in
32 [96].
33
34
35
36
37
38
39
40
41

42 This comparison suggested that the choice of a texturing method is mainly based in
43 the following criteria: simplicity of the texturing technique, commercial availability,
44 equipment cost, texturing cost, texturing speed, minimum size of the individual features
45 that compose the texture pattern, minimum and maximum depth of the features, and
46 limitations in terms of the substrates to be textured: material, shape and size.
47
48
49
50
51
52
53
54
55
56
57
58
59
60

1
2
3
4
5
6
7
8
9 Three alternative surface texturing techniques emerged as potential techniques to be
10 used in some tribological applications, and were experimentally implemented. The first
11 technique, called photochemical texturing, has been widely used and described in the
12 literature, but this work presents some alternatives that reduce equipment and texturing
13 cost. It is a very versatile technique in terms of shapes and patterns of the textures. The
14 second method, called maskless electrochemical texturing (MECT), is potentially rapid
15 and cheap, but the size and shape of the individual features produced is more limited.
16 The third process involves masking the surface by inkjet printing, followed by chemical
17 etching.
18
19
20
21
22
23
24
25
26
27
28
29
30
31

32 **3. Investigation of innovative surface texturing methods**

33
34 The main characteristics of the three alternative texturing techniques that were
35 experimentally investigated will be described, trying to identify their current limitations,
36 particularly in terms of the dimensions of the features that compose the texture. Then, in
37 section 4, the tribological performance of surfaces textured using such methods will be
38 discussed, correlating this performance with the minimum dimensions achievable by
39 each technique.
40
41
42
43
44
45
46
47

48 ***Photochemical texturing (PCT)***

49 This texturing method consists of masking a steel surface by photolithography,
50 followed by chemical etching. It has been used to texture steel surfaces to improve their
51
52
53
54
55
56
57
58
59
60

1
2
3
4
5
6
7
8
9 performance in lubricated contacts [56, 57, 97], but the approach used here is
10 significantly simplified when compared with conventional photolithography. A normal
11 laboratory bench is used, which greatly reduces the complexity and costs of the process
12 in comparison to use of a clean room. **In order to extend this technique to an industrial
13 environment, a clean workspace environment with controlled yellow illumination would
14 be needed, since the photo-resist resin is not sensitive to light of this wavelength.**

15
16
17
18
19
20
21
22 A sample spinner with maximum rotational speed of 7000 rpm was used to ensure
23 the formation of a thin and even resist layer on the steel plate surface. A conventional
24 hot plate was used to bake the samples. A tungsten filament microscope light was used
25 as a source of UV light to expose the resist. Various experimental conditions were tried,
26 based on recommendations found in the literature [98].

27
28
29
30
31
32
33 Before texturing, the samples were cleaned in acetone in an ultrasonic bath. The
34 photoresist (AZ 5214, manufactured by AZ Electronic Materials) was spun on to the
35 surface. The coated sample was then pre-baked. The patterns were designed using
36 Adobe Photoshop software and printed on to A4 paper using a laser printer. They were
37 then photographed to make the masks to be used during the exposure of the resist. This
38 reduced the cost and time that would be involved in the production of conventional
39 metallic masks. **However, the maximum area that could be textured was 35 x 35 mm,
40 which corresponds to the size of the photographic films.** Another route which could
41 probably give adequate resolution would be to print the pattern at the right size directly
42
43
44
45
46
47
48
49
50
51
52
53
54
55
56
57
58
59
60

1
2
3
4
5
6
7
8
9 on to transparent film, by laser or inkjet methods. This would avoid the photographic
10 step and would also increase the size of the area to be textured. However, it would also
11 require a more powerful UV source covering a larger area. There would be challenges
12 in treating components with large areas, above around 250 x 250 mm, with a single
13 exposure using this technique.
14
15
16
17
18
19

20 The exposure to UV light was made by contact printing. After exposure, the samples
21 were developed in AZ 351B developing solution and then post-baked to guarantee
22 complete development of the resist. A 10% aqueous nitric acid solution was used to etch
23 the steel samples at room temperature. The depth of the features was varied by changing
24 the etching time. After etching, the resist was stripped in acetone at room temperature.
25
26
27
28
29

30 Photolithographic resists may be negative or positive. In positive resists,
31 photochemical reactions caused by UV exposure weaken the polymer by scission of the
32 main and side polymer chains. Thus, the exposed areas will be more soluble in
33 developing solutions. Negative resists are strengthened by UV exposure, which
34 promotes random cross-linking of the main or side of the resist. The exposed areas of
35 the resist will be then less soluble in developing solutions. In this work, the use of
36 different UV light sources allowed the same resin to be used as both a negative
37 photoresist (using a lower power light source) and a positive photoresist (using a higher
38 power light source). The conditions used for both conditions varied slightly, as
39 summarized in Table I.
40
41
42
43
44
45
46
47
48
49
50
51
52
53
54
55
56
57
58
59
60

1
2
3
4
5
6
7
8
9
10
11
12
13
14
15
16
17
18
19
20
21
22
23
24
25
26
27
28
29
30
31
32
33
34
35
36
37
38
39
40
41
42
43
44
45
46
47
48
49
50
51
52
53
54
55
56
57
58
59
60

This technique is very versatile in terms of the shapes of the features, which depends on the pattern printed on the masks. The resolution of this simplified procedure is worse than that obtained with conventional photolithography, but obviously depends on the resolution of the mask. For the conditions used in this work, the smallest features that could be produced with good repeatability were circular pockets with an average diameter of $20 \pm 1 \mu\text{m}$.

In Figure 3, examples of the textures generated with the positive resist (pockets) and the negative resist (pillars) are shown. This technique was also used to produce linear and chevron-like grooves, as described in [4].

Maskless electrochemical texturing (MECT)

This is a simple method for texturing metallic surfaces by electrochemical machining, termed ‘maskless electrochemical texturing’ (MECT). It allows a single cathode tool, in which the texture is incorporated through a pattern of perforations, to be used for many texturing operations and avoids the need for masks to be applied to individual workpieces. It therefore has significant advantages over conventional methods of texturing by electrochemical machining that involve prior masking [58, 99]. Locating the electrical insulation that localizes the machining action at the surface of the cathodic tool, instead of applying a mask to each individual workpiece, has been used previously by other authors. Schönenberger and Roy [59] transferred features in the size range from 50 to 200 μm from a patterned cathode tool onto a copper workpiece.

1
2
3
4
5
6
7
8
9 However, the approach in the present work is different, because the electrolyte flows
10 through small perforations on the textured tool which define the pattern to be
11 transferred, ensuring effective cleaning of the tool during machining. The quantity of
12 electrolyte used to machine each workpiece is quite small and the whole apparatus is
13 relatively simple. Finally, it is well suited for the treatment of quite large areas
14 (typically cm^2 to dm^2). Nelson and Schwartz [33] have developed a process called
15 electrochemical printing (ECP), which has some similarities but electrolytically deposits
16 material rather than removing it. Furthermore, the process occurs at a single location
17 rather than over a large number of areas in parallel. Another different configuration has
18 also been used to texture steel surfaces using electrochemical machining without
19 previous masking, but each pocket is produced individually, which substantially
20 increases the texturing time [60].
21
22
23
24
25
26
27
28
29
30
31
32
33
34

35 During texturing, the potential difference between anode and cathode is switched,
36 and consists of brief working pulses (t_p), where anodic dissolution of the workpiece
37 occurs, separated by intervals of duration t_o , where the electrolytic cell is at rest, and the
38 products of anodic dissolution are flushed away from the inter-electrode gap.
39
40
41
42
43

44 Textured carbon steel samples could be produced using this technique with high
45 current efficiencies as described elsewhere [71], and the process was characterized in
46 terms of the effects of current pulse history and electrolyte flushing conditions on
47 current efficiency, material removal rate and feature definition. The variables were the
48
49
50
51
52
53
54
55
56
57
58
59
60

1
2
3
4
5
6
7
8
9 machining time, the pulse length, the pressure of the electrolyte and the separation
10 between the polymer mask plate and the workpiece, obtained by the use of spacers with
11 different thicknesses. Due to its simplicity and low cost, the technique has been
12 investigated by other authors, who used FEM to model the technique [72].
13
14

15
16
17 Subsequently, micro EDM was used to texture the covers of the tools used for
18 MECT, which enabled more complex features to be produced [100]. Also, the
19 technique was optimized in terms of voltage applied between tool and specimen. AISI
20 420 stainless steel tool covers 0.5 mm in thickness were machined by die sinking EDM.
21
22
23

24
25
26 Patterns containing regularly spaced circular dots, arrays of chevrons and parallel
27 arrays of dashed lines with dots could be obtained. To produce the array of dots, a
28 tungsten wire with a diameter of 110 μm was used. For the array of chevrons, copper
29 sheets with thickness of 100 μm were cut to create individual chevron-like features. The
30 dashed lines with dots were produced using the copper sheets and the tungsten wires.
31
32
33
34
35
36
37
38
39 After machining the tool covers, they were covered with an insulating lacquer.

40
41 Polished carbon steel workpieces were textured using various machining conditions.
42 A combination of optimum texturing speed and accuracy was obtained for a gap
43 between tool and specimen of 100 μm , voltages between 30 and 40V, $t_p = 2.5$ ms and t_o
44 = 20 ms. Figure 4 shows an example of textured carbon steel workpieces with different
45
46
47
48
49
50
51
52
53
54
55
56
57
58
59
60
61
62
63
64
65
66
67
68
69
70
71
72
73
74
75
76
77
78
79
80
81
82
83
84
85
86
87
88
89
90
91
92
93
94
95
96
97
98
99
100
101
102
103
104
105
106
107
108
109
110
111
112
113
114
115
116
117
118
119
120
121
122
123
124
125
126
127
128
129
130
131
132
133
134
135
136
137
138
139
140
141
142
143
144
145
146
147
148
149
150
151
152
153
154
155
156
157
158
159
160
161
162
163
164
165
166
167
168
169
170
171
172
173
174
175
176
177
178
179
180
181
182
183
184
185
186
187
188
189
190
191
192
193
194
195
196
197
198
199
200
201
202
203
204
205
206
207
208
209
210
211
212
213
214
215
216
217
218
219
220
221
222
223
224
225
226
227
228
229
230
231
232
233
234
235
236
237
238
239
240
241
242
243
244
245
246
247
248
249
250
251
252
253
254
255
256
257
258
259
260
261
262
263
264
265
266
267
268
269
270
271
272
273
274
275
276
277
278
279
280
281
282
283
284
285
286
287
288
289
290
291
292
293
294
295
296
297
298
299
300
301
302
303
304
305
306
307
308
309
310
311
312
313
314
315
316
317
318
319
320
321
322
323
324
325
326
327
328
329
330
331
332
333
334
335
336
337
338
339
340
341
342
343
344
345
346
347
348
349
350
351
352
353
354
355
356
357
358
359
360
361
362
363
364
365
366
367
368
369
370
371
372
373
374
375
376
377
378
379
380
381
382
383
384
385
386
387
388
389
390
391
392
393
394
395
396
397
398
399
400
401
402
403
404
405
406
407
408
409
410
411
412
413
414
415
416
417
418
419
420
421
422
423
424
425
426
427
428
429
430
431
432
433
434
435
436
437
438
439
440
441
442
443
444
445
446
447
448
449
450
451
452
453
454
455
456
457
458
459
460
461
462
463
464
465
466
467
468
469
470
471
472
473
474
475
476
477
478
479
480
481
482
483
484
485
486
487
488
489
490
491
492
493
494
495
496
497
498
499
500
501
502
503
504
505
506
507
508
509
510
511
512
513
514
515
516
517
518
519
520
521
522
523
524
525
526
527
528
529
530
531
532
533
534
535
536
537
538
539
540
541
542
543
544
545
546
547
548
549
550
551
552
553
554
555
556
557
558
559
560
561
562
563
564
565
566
567
568
569
570
571
572
573
574
575
576
577
578
579
580
581
582
583
584
585
586
587
588
589
590
591
592
593
594
595
596
597
598
599
600
601
602
603
604
605
606
607
608
609
610
611
612
613
614
615
616
617
618
619
620
621
622
623
624
625
626
627
628
629
630
631
632
633
634
635
636
637
638
639
640
641
642
643
644
645
646
647
648
649
650
651
652
653
654
655
656
657
658
659
660
661
662
663
664
665
666
667
668
669
670
671
672
673
674
675
676
677
678
679
680
681
682
683
684
685
686
687
688
689
690
691
692
693
694
695
696
697
698
699
700
701
702
703
704
705
706
707
708
709
710
711
712
713
714
715
716
717
718
719
720
721
722
723
724
725
726
727
728
729
730
731
732
733
734
735
736
737
738
739
740
741
742
743
744
745
746
747
748
749
750
751
752
753
754
755
756
757
758
759
760
761
762
763
764
765
766
767
768
769
770
771
772
773
774
775
776
777
778
779
780
781
782
783
784
785
786
787
788
789
790
791
792
793
794
795
796
797
798
799
800
801
802
803
804
805
806
807
808
809
810
811
812
813
814
815
816
817
818
819
820
821
822
823
824
825
826
827
828
829
830
831
832
833
834
835
836
837
838
839
840
841
842
843
844
845
846
847
848
849
850
851
852
853
854
855
856
857
858
859
860
861
862
863
864
865
866
867
868
869
870
871
872
873
874
875
876
877
878
879
880
881
882
883
884
885
886
887
888
889
890
891
892
893
894
895
896
897
898
899
900
901
902
903
904
905
906
907
908
909
910
911
912
913
914
915
916
917
918
919
920
921
922
923
924
925
926
927
928
929
930
931
932
933
934
935
936
937
938
939
940
941
942
943
944
945
946
947
948
949
950
951
952
953
954
955
956
957
958
959
960
961
962
963
964
965
966
967
968
969
970
971
972
973
974
975
976
977
978
979
980
981
982
983
984
985
986
987
988
989
990
991
992
993
994
995
996
997
998
999
1000

1
2
3
4
5
6
7
8
9 The removal rate in PCT obviously depends on the current density. The use of higher
10 current densities increases the material removal rate, but it can reduce efficiency of
11 metal dissolution. Moreover, since the tests used pulsed current, the removal rate also
12 depends on the duty cycle, defined as the ratio t_{on}/t_{off} . Typical values of machined depth
13 / time obtained for a duty cycle of 0.15 and a current density of 0.85 A.mm^{-2} were
14 around $0.5 \text{ }\mu\text{m.s}^{-1}$.
15
16
17
18
19
20
21

22 ***Masking by inkjet printing***

23
24 In principle, ink-jet printing can provide a method to deposit masks to be used in
25 conjunction with etching for the texturing of engineering surfaces [101]. In early work,
26 Muhl and Alder [102] used a continuous ink-jet printhead with a solvent-based ink to
27 deposit mask patterns on to steel rolls; the deposited drop diameter was $\sim 150 \text{ }\mu\text{m}$. This
28 process, which could readily be extended to other engineering components, was
29 patented [103]. More recently, James [101] discussed the advantages and disadvantages
30 of several ink types for such masking applications, and reported the printing of 120 to
31 150 μm features on metallic substrates with a UV-cured ink. The present work used two
32 different drop-on-demand printers for masking steel surfaces, followed by chemical
33 etching. The first was an industrial flatbed printer (Inca Eagle) with 16 Spectra SE
34 printheads each 128 nozzles, and UV-curable inks. The physical distance between the
35 nozzles gives a printing resolution of 50 dpi (dots per inch) in the direction
36 perpendicular to the printing direction. The use of more than one printhead can enhance
37
38
39
40
41
42
43
44
45
46
47
48
49
50
51
52
53
54
55
56
57
58
59
60

1
2
3
4
5
6
7
8
9 the resolution. For conventional graphics printing each colour (cyan, magenta, yellow
10 and black) can be printed using up to 4 printheads if all colours are used at once, or up
11 to 16 printheads if monochromatic printing is used. All jets can be fired simultaneously
12 or individually. The nozzle diameter is 38 μm and the calibrated drop size is 30 pl. The
13 second was a Dimatix Materials Printer (DMP-2800) with a nominal 10 pl drop size.
14 The ink was a commercial lactate solvent-based black ink (dye-based, JetStream PCS
15 7561, Sun Chemical) with a viscosity of 12.1 mPa s at 25°C and a surface tension of
16 31.5 mN m⁻¹.
17
18
19
20
21
22
23
24
25

26 For any printing method, to obtain reproducible printing results, it is crucial to
27 control surface cleanliness, since a different wettability of the ink on the surface can
28 result in printing distortions. Various cleaning routines were tried, as described in Table
29 II. Contact angle measurements were performed for each cleaning condition using the
30 sessile drop technique to quantify the efficiency of the cleaning methods. Additionally,
31 a plasma chamber was also tried as a cleaning method, both for a sample that was
32 polished 4 hours before (sample 3_F) and for a sample polished one month before
33 (sample 3_G).
34
35
36
37
38
39
40
41
42
43

44 The best cleaning routine was 3_C (Figure 5), which gave the lowest contact angle
45 and the smallest scatter between different measurements both for inks and for deionized
46 water. Therefore, this cleaning routine was used whenever printing was not carried out
47 immediately after polishing.
48
49
50
51
52
53
54
55
56
57
58
59
60

1
2
3
4
5
6
7
8
9 The influence of substrate surface finish on printing and wettability was studied by
10 comparing highly polished steel surfaces and surfaces ground with silicon carbide paper
11 with three different grit sizes (800, 320 and 120 mesh). After grinding, the surfaces
12 were rinsed with acetone and dried in air. Wettability for each surface condition was
13 assessed in terms of contact angles for the solvent-based ink. The surface finishing step
14 was performed immediately before the contact angle measurements.
15
16
17
18
19
20
21

22 Figure 6 shows that the increase of surface roughness reduced the **apparent** contact
23 angle, probably due to the spreading of the ink within the surface grooves, which was
24 observed for all the printings on roughened surfaces. **According to the Wenzel's model,**
25 **static contact angle measurements using a drop that is substantially larger than the**
26 **roughness scale should indeed give larger values for rough surfaces when compared**
27 **with a smooth surface if the solid is hydrophilic [104]. The apparent contact angle,**
28 **which contains contributions both from the surface roughness and from any changes in**
29 **the true, local contact angle resulting from chemical modification of the surface,**
30 **controls the spreading of the ink drop.** Therefore, it was concluded that roughening the
31 surface could not be used to reduce the minimum size of the ink droplets on these metal
32 samples.
33
34
35
36
37
38
39
40
41
42
43
44
45

46 One set of experiments using the DMP printer and solvent-based inks explored the
47 whole texturing process, including the etching behavior and methods for stripping the
48 resist. After printing of individual dots, the masked samples were etched with aqueous
49
50
51
52
53
54
55
56
57
58
59
60

1
2
3
4
5
6
7
8
9 nitric acid at various concentrations for different periods of time. After etching, the ink
10 deposits were stripped by immersion in acetone with ultrasonic agitation at 25 °C. The
11 samples were examined by optical microscopy before etching, after etching and after
12 stripping. The surface topography of the textured samples was assessed by laser
13 interferometry.
14
15
16
17
18

19 Figure 7(a) shows that the smallest features that could be printed with the DMP
20 printer on polished steel were a pattern of circular dots (diameter ~ 60µm), where each
21 dot was formed by a single droplet with an ejected ink drop diameter of 27 µm. Optimal
22 etching behavior was found for a nitric acid concentration of 5%. The ink protected the
23 steel surface during etching and was easily stripped by ultrasonic cleaning in acetone.
24 Figure 7(b) shows a 3D map of the final textured surface. The diameters of the unetched
25 islands for an etching time of 5 minutes in 5% nitric acid were ~50 µm, suggesting that
26 the extent of the undercutting was ~5 µm per edge, and the depth was ~ 3 µm (Figure
27 7(c)).
28
29
30
31
32
33
34
35
36
37
38

39 However, the textures shown above are composed of a regular array of pillar-like
40 shapes. For tribological applications in lubricated sliding, the best results have been
41 shown for patterns composed of pocket-like or groove-like shapes. Therefore, other sets
42 of experiments were carried out to investigate how patterns composed of regular arrays
43 of gaps could be printed on a steel surface, with both a flatbed Eagle printer using UV-
44 curable inks and a DMP-2800 printer using solvent-based inks.
45
46
47
48
49
50
51
52
53
54
55
56
57
58
59
60

1
2
3
4
5
6
7
8
9 The tests with the flatbed printer were carried out using different numbers of
10 printheads, printing speeds and resolutions, to identify printing routines able to produce
11 patterns that could potentially be used in tribological applications. Some successful
12 examples are shown in Figure 8. Parallel linear gaps of $22 \pm 5 \mu\text{m}$ could be printed with
13 1000 dpi resolution (a). When square gaps were printed, their shape varied between
14 adjacent rows of squares and repeated at every four rows, which is the number of
15 printheads used to give the resolution of 1000 dpi. Interrupted lines (c) and chevron-like
16 features (d and e) could also be produced. When printing was carried out in a single
17 step, using four printheads simultaneously, the shape of the chevrons was more irregular
18 (d), but the size of the chevrons was smaller than when printing was carried out in
19 multiple steps, using one individual printhead (e).
20
21
22
23
24
25
26
27
28
29
30
31
32

33 For printing complex-shape patterns with the DMP-2800 printer using solvent-based
34 ink, AISI 1010 steel samples were used as substrates. The minimum width that could be
35 achieved when linear parallel gaps were printed was $20 \mu\text{m}$ (Figure 9(a)). More
36 complex shapes, such as square gaps (b) and chevrons (c) showed some distortion and
37 the minimum size of the features was larger. Another interesting feature of printing with
38 the solvent-based ink was that, although it was black, the thin printed films on a highly
39 reflective steel substrate showed a clear pattern of coloured interference fringes. Surface
40 topography measurements of the ink deposits showed that the colours could be
41 associated with the thickness of the ink. After calibration, this provided a simple and
42
43
44
45
46
47
48
49
50
51
52
53
54
55
56
57
58
59
60

1
2
3
4
5
6
7
8
9 reliable method to evaluate dry film thickness. This effect was not observed with the
10 UV-curable ink (Figure 8), probably because of the reduced spreading after printing.
11

12 *Summary of the texturing methods*

13
14 This paper presents three alternative surface texturing methods that successfully
15 produced texturing patterns on steel surfaces composed of: parallel grooves, regular
16 arrays of dots (circular or square pockets), and regular arrays of chevrons, as shown
17 schematically in Figure 10.
18
19

20
21 The methods present different characteristics, which should affect their suitability as
22 a texturing technique for a certain tribological application. Some comparison between
23 them is necessary to help users. The comparison criteria in this work were chosen from
24 the database described in section 2. Since laser texturing is undoubtedly the most
25 successful commercial texturing technique, consideration of alternative texturing
26 techniques should include a comparison with laser texturing. However, this poses
27 problems, since the performance of commercial laser texturing facilities can vary
28 significantly.
29
30

31
32 If the maximum pulse energy of a laser system is higher than the ablation threshold
33 fluence for the target material, a stationary laser beam with a spot comparable to the
34 pocket diameter can be used to create an array of pockets without the need for laser spot
35 scanning [28]. Small beam spot sizes result in a higher maximum energy, but require
36 more sophisticated optics.
37
38
39
40
41
42
43
44
45
46
47
48
49
50
51
52
53
54
55
56
57
58
59
60

1
2
3
4
5
6
7
8
9
10
11
12
13
14
15
16
17
18
19
20
21
22
23
24
25
26
27
28
29
30
31
32
33
34
35
36
37
38
39
40
41
42
43
44
45
46
47
48
49
50
51
52
53
54
55
56
57
58
59
60

Studies can be found in the literature regarding the correlation between the number of pulses and the depth of the pockets. For example, for a nanosecond (ns) laser without laser spot scanning, when the number of consecutive pulses on the same spot varied from 3 to 20, a pocket was progressively machined. This work showed that with around 10 pulses, pocket depths of around 20 μm were obtained when pulse energies between 3.7 and 8.3 mJ during texturing of 100Cr6 steel samples, with small lateral damage [105]. The use of shorter pulses, besides producing small heat-affected zones, also reduces even further the time necessary to machine each pocket.

Among typical lasers, ns pulsed lasers present a good compromise between relatively short pulse duration and a reasonable cost, and hence are widely used in industrial applications [28]. However, the use of ultrashort pulses (femtosecond lasers) combined with small beam spots and high laser energy may allow higher texturing speeds.

In Table III, these methods are summarized in terms of cost and complexity, restrictions and texturing speed. For comparison, estimates are also presented for laser texturing (LT). Due to the large variability between lasers, two rough estimates are presented, one for a more standard nanosecond laser and another for a femtosecond laser with more sophisticated optics. The texturing speed was estimated as the approximate time necessary to texture a clean smooth area of 100 x 100 mm. Only the time necessary for masking of the surfaces (if necessary) and to machine the pockets was computed, excluding time needed for setting up the equipment or for any pre/post

1
2
3
4
5
6
7
8
9
10
11
12
13
14
15
16
17
18
19
20
21
22
23
24
25
26
27
28
29
30
31
32
33
34
35
36
37
38
39
40
41
42
43
44
45
46
47
48
49
50
51
52
53
54
55
56
57
58
59
60

treatment. The texture pattern was composed of an array of pockets with diameter of 100 μm and an area coverage of 25%, which gives a total of 27889 pockets. Since the pockets are produced in a serial manner, either an x - y stage moves the sample or the laser beam is steered for each pocket to be produced. Considering recent advances in commercial positioning stages and the very high speed for laser steering in modern laser facilities, it is estimated that the time to produce each pocket may vary between 1 to 10 ms for femtosecond laser with sophisticated optics and between 50 to 100ms for standard nanosecond lasers. Therefore, the time necessary to machine 27889 pockets must be in the range from 30 s to 5 min for more sophisticated lasers and in the range from 20 to 45 minutes. It is important to emphasize that the values presented here for all the texturing techniques are only rough approximations, based on the current state of development of each technique.

The main advantage of PCT is its flexibility in terms of the shapes of the individual features. The resolution is comparable to that obtained by most commercial laser texturing facilities, although worse than the resolution of more sophisticated laser facilities. Despite the time required to mask the individual surfaces to be textured, it can be faster than laser texturing for large texturing areas, because the texturing time is independent of the area coverage.

MECT is very cheap and fast, but it can only texture surfaces with good electrical conductivity and reactivity, where a suitable anodic dissolution reaction can be

1
2
3
4
5
6
7
8
9 achieved. The resolution is worse than that of laser texturing, although it is believed that
10 the use of other techniques to produce the tool (in particular, laser machining) could
11 help to reduce the minimum size of the features.
12
13

14
15 Masking by inkjet printing showed better resolution than MECT, but was inferior to
16 laser texturing. Texturing results have been demonstrated for flat surfaces, but in
17 principle the technique could also be extended to curved surfaces [47]. Despite the time
18 necessary to mask each individual workpiece, the speed of the technique is still possibly
19 faster than laser texturing, depending on the characteristics of the laser texturing
20 facilities.
21
22
23
24
25
26
27
28

29 **4. Tribological performance**

30 *Hydrodynamic lubrication*

31
32 The summary presented in Table III shows that despite the simplifications introduced
33 during the photolithographic masking of metal surfaces, fairly small and well-controlled
34 features could be produced by PCT. This suggested that it could be well suited to
35 texture sliding surfaces under hydrodynamic lubrication. To investigate this hypothesis,
36 results from reciprocating sliding tests (stroke length = 22 mm and frequency = 0.55
37 Hz) carried out between smooth stationary cylindrical counterbodies and plane samples
38 textured by PCT [4] are analyzed. The tests used two different counter-bodies: a mirror-
39 polished, 8 mm radius brass cylinder and a mirror-polished sector of a 100 mm radius
40 aluminum alloy cylinder, both aligned perpendicularly to the sliding direction. Flooded
41
42
43
44
45
46
47
48
49
50
51
52
53
54
55
56
57
58
59
60

1
2
3
4
5
6
7
8
9 lubrication conditions with a highly viscous additive-free mineral oil (dynamic viscosity
10 of 1.5 Pa s at 20 °C), associated with a large cylinder radius, were used to ensure
11 hydrodynamic lubrication conditions despite the non-conformal contact geometry. The
12 geometrical characteristics of selected textured samples, measured by laser
13 interferometry, are shown in Table IV. Table V shows the loads and the corresponding
14 elastic contact pressures (p) and contact widths ($2a$) calculated from the Hertz equation
15 for a line contact (length of the cylinder = 16 mm). The texture geometries and normal
16 loads were chosen to allow the ratio between the contact width and the size of the
17 individual features that compose the texture pattern to be varied. No wear was
18 detectable by optical examination of the cylinder or plane specimens after the tests,
19 except at the ends of the strokes, suggesting that they did indeed operate with the
20 hydrodynamic lubrication regime.
21
22
23
24
25
26
27
28
29
30
31
32
33
34

35 Capacitance measurements were used to evaluate film thickness, as described in [4].
36 After running-in, points from consecutive cycles corresponding to the same translational
37 velocity were then averaged, to compute mean values of film thickness for an average
38 stroke.
39
40
41
42
43

44 For the cylinder with smaller diameter and therefore narrower contact widths, the
45 ratio between the pocket diameter and the contact width (d/CW) varied between 2 and
46 8.5, i.e., the pockets were substantially wider than the contact. For those cases, film
47 thickness was reduced when compared with a smooth surface, as exemplified in Figure
48
49
50
51
52
53
54
55
56
57
58
59
60

1
2
3
4
5
6
7
8
9 11 (a). On the other hand, for a cylinder diameter of 200 mm, d/CW reduced to between
10
11 0.5 and 1, so that the pockets were normally narrower than the contact. For those cases,
12
13 surface texturing could lead to increased film thickness for some texturing geometries,
14
15 as exemplified in Figure 11(b), which compares film thickness as a function of the
16
17 fraction of area coverage (f), for samples containing circular features.
18
19

20 Further details of the effect of the texture geometries on film thickness and friction
21
22 coefficient can be found in [4]. The results presented in this reference show that
23
24 chevron-like pockets and parallel lines oriented perpendicular to the sliding direction
25
26 can be particularly beneficial under certain sliding conditions, emphasizing the
27
28 importance of texturing methods that are flexible in terms of the geometry of the texture
29
30 patterns. However, it is important to emphasize that although the potential for texture to
31
32 increase load support and reduce friction can often justify the effort and cost, in
33
34 particular for hydrodynamic bearings [16], poorly chosen texture geometries or
35
36 operating conditions can result in decreased load capacity.
37
38

39 From the alternative texturing methods presented here, PCT would be in principle the
40
41 best suited for hydrodynamic applications, since it can produce the smallest features.
42
43 However, it is not the absolute size of the features that is decisive in the choice of the
44
45 adequate texturing method, but their relative size in relation to the operating conditions.
46
47 For example, Fowell et al. [16] suggest the non-dimensional parameter $TS = a/B$, where
48
49 a is the distance from the inlet to the first pocket and B is the pocket width, to take
50
51
52
53
54
55
56
57
58
59
60

1
2
3
4
5
6
7
8
9 account of the width of the pocket, and the two parameters $TH = h/B$, where h is the
10 height of the pockets and $MH = h_o/B$, where h_o = minimum oil film thickness, to take
11 account of the depth of the pockets. Also, they suggest that the effect of number of
12 pockets on the performance of a textured hydrodynamic bearing is minimal. This means
13 that if the total area of the pockets ensures that the desired area coverage is obtained, a
14 texturing method that generates fewer wider pockets could be adequate.
15
16
17
18
19
20
21

22 Therefore, for hydrodynamic applications where contact widths and minimum film
23 thickness are large, such as in the case of large hydrodynamic bearings, larger pockets
24 could be used successfully, and therefore MECT and masking by inkjet printing could
25 also be alternatives. They would be particularly advantageous considering the size of
26 the areas to be textured, where the texturing time could become excessively large for
27 laser texturing.
28
29
30
31
32
33
34

35 ***Starved lubrication***

36
37
38 The tribological performance of the textured surfaces was also evaluated under
39 conditions of starved lubrication. This condition was chosen because the pockets that
40 compose the texture are also expected to act as reservoirs for lubricant when the supply
41 of lubricant is limited. In previous work, we have shown that this was the case for
42 texturing dies used in strip drawing. Patterned dies showed reduced friction and resulted
43 in better surface finish on the drawn strip when compared with smooth dies [13].
44
45
46
47
48
49
50
51
52
53
54
55
56
57
58
59
60

1
2
3
4
5
6
7
8
9 In the present work, the effect of surface texturing was analyzed for reciprocating
10 sliding tests under starved liquid lubrication conditions. MECT was chosen as the
11 texturing method because it resulted in the largest features from the three methods
12 proposed. Flat carbon steel samples were textured with arrays of circular pockets ($d =$
13 $190 \mu\text{m}$, $p_x = 320 \mu\text{m}$, $h = 10 \mu\text{m}$). For comparison, the smooth areas between pockets
14 for a textured sample ($S_q = 0.590 \mu\text{m}$) were tested under similar conditions (termed
15 ‘smooth surface’). In order to guarantee enough area between the pockets to be tested
16 for the smooth surface, p_x was increased to 1.4 mm in the comparison sample. Despite
17 the narrow contact widths, special care was taken to position the wear track precisely
18 over a line of pockets for the textured samples and between lines of pockets for the
19 smooth sample.
20
21
22
23
24
25
26
27
28
29
30
31
32

33 Very small quantities of a naphthenic oil without anti-wear additives (viscosity at
34 $40^\circ\text{C} = 0.026 \text{ Pa s}$) were applied to the surface samples with a micropipette before
35 reciprocating sliding tests. Different normal loads were used and therefore the ratio
36 between the pocket diameters and the contact width (d/CW) varied (Table VI).
37
38
39
40
41

42 AISI 52100 steel balls ($\phi = 10 \text{ mm}$) were used as counterbodies. Three repetitions
43 were carried out for each condition. Friction force was continuously monitored with a
44 high frequency acquisition system to allow the acquisition of many points within each
45 stroke. To facilitate the visualization and interpretation of the data, a program
46 developed in Matlab was used to generate a triboscopic map of the variables during the
47
48
49
50
51
52
53
54
55
56
57
58
59
60

1
2
3
4
5
6
7
8
9 tests, where z is friction coefficient, x is the position of the counterbody within each
10 cycle of test and y is the number of the test cycle.

11
12
13 Figure 12 shows triboscopic maps for friction coefficients obtained for textured (left)
14 and smooth (right) surfaces. In all maps, some peaks can be observed for the friction
15 coefficients. This suggests that for the starved lubrication regime used in this work, the
16 lubrication failed at some points of the surface, probably due to inability of the lubricant
17 to refill the inlet after each pass, and that at the regions where the lubricant was present,
18 friction coefficient was lower. For the smaller normal load of 2.5N, friction coefficients
19 were high for a lubricated contact. It is believed that for such low load, the load cell
20 used to measure friction force (range = 1000 N) was not sensitive enough. However, all
21 three tests for each sample at this load repeated the behaviours exemplified in (a) and
22 (b). The difference between the smooth and the textured samples is not large, but for the
23 textured samples, the friction peaks were much less frequent than for the smooth
24 samples.
25
26
27
28
29
30
31
32
33
34
35
36
37
38

39 For the loads of 12.74 and 51.94 N, the friction coefficient was larger at the ends of
40 each stroke for all samples. Examples are shown in (c) for the textured sample and (d)
41 for smooth samples at 51.94 N. This might suggest that at those locations, where the
42 speed is virtually zero, combined with the higher contact pressures and the starved
43 lubrication conditions, lubrication failure was more significant. Also, wear debris
44 tended to accumulate at the ends of the strokes. On the other hand, at the regions distant
45
46
47
48
49
50
51
52
53
54
55
56
57
58
59
60

1
2
3
4
5
6
7
8
9 from the ends of the stroke, friction coefficient was lower for the textured sample,
10 suggesting better lubrication. Under high normal loads, starvation is expected to be
11 more severe. Also, the contact is wider, so that the pockets are fully contained within
12 the contact. It is believed that under these conditions, the lubricant within the pockets is
13 helping to replenish the contact inlet for the next cycle, reducing friction coefficient.
14
15 However, despite the high acquisition rate used to sample friction force, localized
16 friction reduction that repeated with a frequency proportional to the distance between
17 the pockets could not be detected.
18
19

20
21
22
23
24
25
26 SEM of the wear tracks showed that they were wider than the diameter of the pockets
27 for the lowest load (Figure 13), despite the pockets being wider than the elastic contact
28 width ($d/CW = 2.1$). This might justify the occurrence of some positive effect of the
29 texturing to replenish the contact inlet with lubricant, although it was more significant
30 for smaller values of d/CW . Figure 13 (b) shows wider wear tracks at the ends of the
31 strokes, where friction coefficients had been larger than in the middle of the strokes for
32 the loads of 12.7 and 51.94 N.
33
34
35
36
37
38
39
40
41

42 Those results suggest that for a texturing method to be suitable for applications
43 involving sliding under conditions of limited supply of lubricant, it must be capable of
44 producing features that are narrower than the sliding contact and that the effect is more
45 significant when the ratio between the pocket diameter and the contact width is small.
46
47
48
49
50
51
52
53
54
55
56
57
58
59
60

1
2
3
4
5
6
7
8
9 Therefore, many components that operate under limited lubricant supply could have
10 their performance improved by any of the alternative texturing methods presented here.
11

12
13 Although the effect of the pocket depth was not investigated in this work, the
14 literature [18, 22] suggests that when the pocket depth is very large, surface tension can
15 drive lubricant from the contact to the bottom of the pockets, reducing the lubricant
16 supply in the contact inlet. Such an effect was not observed in our tests, but it was
17 reported during reciprocating sliding tests under mild starvation conditions for $d = 100$
18 μm and $h = 20 \mu\text{m}$ in [18] and much more severely for $d = 125 \mu\text{m}$ and $h = 125 \mu\text{m}$ in
19 [22].
20
21
22
23
24
25
26
27
28
29

30 **5. Conclusions**

31
32 This work investigated the use of alternative surface texturing methods for
33 tribological applications.
34

35
36 Texturing methods were identified and classified into groups and subgroups,
37 according to their physical principles. This included not only methods already existent
38 either in industrial practice or research, but also new possible methods.
39
40
41
42

43
44 Three alternative texturing methods were detailed and investigated, in order to
45 explore their viability, main characteristics, potential and limitations. All three
46 techniques were successfully demonstrated to texture steel surfaces with patterns
47 containing arrays of dots, lines and chevrons.
48
49
50
51
52
53
54
55
56
57
58
59
60

1
2
3
4
5
6
7
8
9 Although photochemical texturing (PCT) is widely used in the electronics industry,
10 the approach used in this work was much simpler and cheaper.

11
12
13 Maskless electrochemical texturing (MECT) is simple, cheap and fast, but the
14 minimum size of the features is still a limitation. It involves the application of a pulsed
15 voltage to an electrochemical cell composed of a textured tool and the workpiece.
16
17

18
19
20 Inkjet printing was used to mask steel surfaces, which were then etched to produce
21 textured surfaces. The resolution was higher than for MECT, but lower than for PCT.
22 The texturing speed depends on surface area, but it is always much slower than MECT.
23
24

25
26
27 A comparison of textured and smooth surfaces under hydrodynamic lubrication in
28 reciprocating sliding showed that for the texturing method to be successful it must be
29 able to produce pockets or grooves that are narrower than the contact width. Therefore,
30 for components with large contacts under hydrodynamic lubrication, such as
31 hydrodynamic bearings, any of the alternative texturing methods could be beneficial if
32 adequate texture geometries are chosen according to the operating parameters.
33
34
35
36
37
38

39
40 A comparison of textured and smooth surfaces under starved lubrication in
41 reciprocating sliding suggested that the pockets helped to replenish the contact with
42 lubricant, reducing friction, in particular when the ratio between the diameter of the
43 pockets and the contact width was low. Again, this suggests that for certain components
44 under starved lubrication, the alternative texturing methods presented here could be
45
46
47
48
49
50
51
52
53
54
55
56
57
58
59
60

beneficial, but this requires the choice of the texture geometry to take into account operating conditions.

6. Acknowledgements

The authors are grateful to Fapemig/Brazil, Capes/Brazil and the Royal Society (UK) for financial support.

7. References

1. Bruzzone, A.A.G., et al., *Advances in engineered surfaces for functional performance*. Cirp Annals-Manufacturing Technology, 2008. **57**(2): p. 750-769.
2. Krupka, I., M. Vrbka, and M. Hartl, *Effect of surface texturing on mixed lubricated non-conformal contacts*. Tribology International, 2008. **41**(11): p. 1063-1073.
3. Rapoport, L., et al., *Friction and wear of MoS(2) films on laser textured steel surfaces*. Surface & Coatings Technology, 2008. **202**(14): p. 3332-3340.
4. Costa, H.L. and I.M. Hutchings, *Hydrodynamic lubrication of textured steel surfaces under reciprocating sliding conditions*. Tribology International, 2008. **40**: p. 1227–1238.
5. Etsion, I., Y. Kligerman, and G. Halperin, *Analytical and experimental investigation of laser-textured mechanical seal faces*. Tribology Transactions, 1999. **42**(3): p. 511-516.
6. Nanbu, T., et al., *Micro-textures in concentrated conformal-contact lubrication: Effects of texture bottom shape and surface relative motion*. Tribology letters, 2008. **29**(3): p. 241-252.
7. Krupka, I. and M. Hartl, *Experimental study of microtextured surfaces operating under thin-film EHD lubrication conditions*. Journal of Tribology-Transactions of the Asme, 2007. **129**(3): p. 502-508.
8. Etsion, I., *State of the art in laser surface texturing*. Journal of Tribology-Transactions of the Asme, 2005. **127**(1): p. 248-253.
9. Krupka, I. and M. Hartl, *The effect of surface texturing on thin EHD lubrication films*. Tribology International, 2007. **40**(7): p. 1100-1110.
10. Ryk, G. and I. Etsion, *Testing piston rings with partial laser surface texturing for friction reduction*. Wear, 2006. **261**(7-8): p. 792-796.
11. Krupka, I., et al., *Effect of surface texturing on elastohydrodynamically lubricated contact under transient speed conditions*. Tribology International, 2011. **44**(10): p. 1144-1150.
12. Mourier, L., et al., *Lubrication mechanisms with laser-surface-textured surfaces in elastohydrodynamic regime*. Proceedings of the Institution of Mechanical Engineers Part J-Journal of Engineering Tribology, 2010. **224**(J8): p. 697-711.
13. Costa, H.L. and I.M. Hutchings, *Effects of die surface patterning on lubrication in strip drawing*. J. Mater. Process. Tech., 2009. **209**(3): p. 1175-1180.

- 1
 - 2
 - 3
 - 4
 - 5
 - 6
 - 7
 - 8
 - 9
 - 10
 - 11
 - 12
 - 13
 - 14
 - 15
 - 16
 - 17
 - 18
 - 19
 - 20
 - 21
 - 22
 - 23
 - 24
 - 25
 - 26
 - 27
 - 28
 - 29
 - 30
 - 31
 - 32
 - 33
 - 34
 - 35
 - 36
 - 37
 - 38
 - 39
 - 40
 - 41
 - 42
 - 43
 - 44
 - 45
 - 46
 - 47
 - 48
 - 49
 - 50
 - 51
 - 52
 - 53
 - 54
 - 55
 - 56
 - 57
 - 58
 - 59
 - 60
14. Pettersson, U. and S. Jacobson, *Friction and wear properties of micro textured DLC coated surfaces in boundary lubricated sliding*. Tribology letters, 2004. **17**(3): p. 553-559.
15. Zumgahr, K.H., M. Mathieu, and B. Brylka, *Friction control by surface engineering of ceramic sliding pairs in water*. Wear, 2007. **263**: p. 920–929.
16. Krupka, I. and M. Hartl, *Effect of Surface Texturing on Very Thin Film EHD Lubricated Contacts*. Tribology Transactions, 2009. **52**(1): p. 21-28.
17. Ausas, R.F., M. Jai, and G.C. Buscaglia, *A Mass-Conserving Algorithm for Dynamical Lubrication Problems With Cavitation*. Journal of Tribology-Transactions of the Asme, 2009. **131**(3).
18. Ryk, G., Y. Kligerman, and I. Etsion, *Experimental investigation of laser texturing for reciprocating automotive engines*. Tribology Transactions, 2002. **45**(4): p. 444-449.
19. Lugt, P.M. and G.E. Morales-Espejel, *A Review of Elasto-Hydrodynamic Lubrication Theory*. Tribology Transactions, 2011. **54**(3): p. 470-496.
20. Chiu, Y.P., *Analysis and Prediction of Lubricant Film Starvation in Rolling Contact Systems*. Asle Transactions, 1974. **17**(1): p. 22-35.
21. Demirci, I., et al., *The Scale Effect of Roughness on Hydrodynamic Contact Friction*. Tribology Transactions, 2012. **55**(5): p. 705-712.
22. Cho, M.H. and S. Park, *Micro CNC surface texturing on polyoxymethylene (POM) and its tribological performance in lubricated sliding*. Tribology International, 2011. **44**(7-8): p. 859-867.
23. Shinkarenko, A., Y. Kligerman, and I. Etsion, *The Effect of Elastomer Surface Texturing in Soft Elasto-Hydrodynamic Lubrication*. Tribology letters, 2009. **36**(2): p. 95-103.
24. Dumitru, G., et al., *Laser microstructuring of steel surfaces for tribological applications*. Applied Physics A, 2000. **70**: p. 485-487.
25. Geiger, M., S. Roth, and W. Becker, *Influence of laser-produced microstructures on the tribological behaviour of ceramics*. Surf. Coat. Technol., 1998. **100-101**: p. 17-22.
26. Semaltianos, N.G., et al., *Femtosecond laser surface texturing of a nickel-based superalloy*. Applied Surface Science, 2008. **255**(5): p. 2796-2802.
27. Vincent, C., et al., *Control of the quality of laser surface texturing*. Microsystem Technologies-Micro-and Nanosystems-Information Storage and Processing Systems, 2008. **14**(9-11): p. 1553-1557.
28. Gao, Y.B., et al., *A two-step nanosecond laser surface texturing process with smooth surface finish*. Applied Surface Science, 2011. **257**(23): p. 9960-9967.
29. Kong, M.C., et al., *On the relationship between the dynamics of the power density and workpiece surface texture in pulsed laser ablation*. Cirp Annals-Manufacturing Technology, 2012. **61**(1): p. 203-206.
30. Duarte, M., et al., *Increasing lubricant film lifetime by grooving periodical patterns using laser interference metallurgy*. Advanced Engineering Materials, 2008. **10**(6): p. 554-558.
31. Kalvala, P.R., D.P. Beesabathina, and K.E. Wiedemann, *Process for forming a wear-resistant coating that minimizes debris*, in USPTO1999, Analytical Services & Mat. Inc.: US.
32. Deng, T., et al., *Fabrication of metallic microstructures using exposed, developed silver halide-based photographic film*. Analytical Chemistry, 2000. **72**(4): p. 645-651.
33. Nelson, J.B. and D.T. Schwartz, *Electrochemical printing: in situ characterization using an electrochemical quartz crystal microbalance*. Journal of Micromechanics and Microengineering, 2005. **15**(12): p. 2479-2484.

- 1
 - 2
 - 3
 - 4
 - 5
 - 6
 - 7
 - 8
 - 9
 - 10
 - 11
 - 12
 - 13
 - 14
 - 15
 - 16
 - 17
 - 18
 - 19
 - 20
 - 21
 - 22
 - 23
 - 24
 - 25
 - 26
 - 27
 - 28
 - 29
 - 30
 - 31
 - 32
 - 33
 - 34
 - 35
 - 36
 - 37
 - 38
 - 39
 - 40
 - 41
 - 42
 - 43
 - 44
 - 45
 - 46
 - 47
 - 48
 - 49
 - 50
 - 51
 - 52
 - 53
 - 54
 - 55
 - 56
 - 57
 - 58
 - 59
 - 60
34. Budinsky, K.G., *Surface Engineering for Wear Resistance* 1988, New York: Prentice Hall. 44-77.
35. Xia, Y. and G.M. Whitesides, *Soft lithography*. *Angew. Chem. Int. Ed.*, 1998. **37**(5): p. 550-575.
36. Vaeth, K.M., et al., *Use of μ CP for generating selectively grown films of poly(p-phenylene vinylene) and parylenes prepared by CVD*. *Langmuir*, 2000. **16**: p. 8495-8500.
37. Wang, H.Y., et al., *Fabrication and electron field-emission of carbon nanofibers grown on silicon nanoporous pillar array*. *Applied Surface Science*, 2012. **261**: p. 219-222.
38. Hupp, S.J. and D.P. Hart. *Quantifying the effect of lubricant elasticity on microtextured surfaces*. in *World tribology congress III*. 2005. Washington: ASME.
39. Bartz, M., et al., *Stamping of monomeric SAMs as a route to structured crystallisation templates: patterned titania films*. *Chem. Eur. J.*, 2000. **6**(22): p. 4149-4153.
40. Mott, M. and J.R.G. Evans, *Zirconia/alumina functionally graded material made by ceramic ink jet printing*. *Mat Sci Eng A*, 1999. **271**: p. 344-352.
41. Snell, D. and A. Coombs, *Novel coating technology for non-oriented electrical steels*. *J Magnetism and Magnetic Mat*, 2000. **215-216**: p. 133-135.
42. Daniel, J.H., D.F. Moore, and J.F. Walker, *Focused ion beams and silicon-on-insulator - a novel approach to MEMS*. *Smart Mater. Struct.*, 2000. **9**: p. 284-290.
43. Hua, M., et al., *Patterned PVD TiN spot coatings on M2 steel: Tribological behaviors under different sliding speeds*. *Wear*, 2006. **260**(11-12): p. 1153-1165.
44. Zou, M., L. Cai, and H. Wang, *Adhesion and friction studies of a nano-textured surface produced by spin coating of colloidal silica nanoparticle solution*. *Tribology Letters*, 2006. **21**(1): p. 25-30.
45. Wuhner, R. and W.Y. Yeung, *Grain refinement with increasing magnetron discharge power in sputter deposition of nanostructured titanium aluminium nitride coatings*. *Scripta Materialia*, 2004. **50**(6): p. 813-818.
46. Lejeune, M., et al., *Ink-jet printing of ceramic micro-pillar arrays*. *Journal of the European Ceramic Society*, 2009. **29**(5): p. 905-911.
47. Hutchings, I.M. and G.D. Martin, eds. *Inkjet technology for digital fabrication*. 2013, Wiley.
48. Pawelski, O., et al., *The influence of different work-roll texturing systems on the development of surface structure in the temper rolling process of steel sheet used in the automotive industry*. *Journal of Materials Processing Technology*, 1994. **45**: p. 215-222.
49. Sheu, S. and L.G. Hector Jr., *Tool surface topographies for controlling friction and wear in metal-forming processes*. *Transactions of ASME, Journal of Tribology*, 1998. **120**: p. 517-527.
50. Mailis, S., et al., *Etching and printing of diffractive optical microstructures by a femtosecond excimer laser*. *Applied Optics*, 1999. **38**(11): p. 2303-2308.
51. Wakuda, M., et al., *Effect of surface texturing on friction reduction between ceramic and steel materials under lubricated sliding contact*. *Wear*, 2003. **254**(3-4): p. 356-363.
52. Fu, Y.H., et al., *The technology of laser honing applied in distinctively improving the lubrication of frictional units*. *Key Engineering Materials*, 2001. **202-203**: p. 265-270.
53. Aspinwall, D.K., et al., *Electrical Discharge Texturing*. *J. Mach. Tools Manufact.*, 1992. **32**(12): p. 183-193.
54. De Soete, D., D. Pans, and K. Steinhoff, *EBT technology and its applications*. *Iron and Steel Engineering*, 1997(September): p. 36-40.

- 1
2
3
4
5
6
7
8
9
10
11
12
13
14
15
16
17
18
19
20
21
22
23
24
25
26
27
28
29
30
31
32
33
34
35
36
37
38
39
40
41
42
43
44
45
46
47
48
49
50
51
52
53
54
55
56
57
58
59
60
55. Langford, R.M., et al., *Focused ion beam micromachining of three-dimensional structures and three-dimensional reconstruction to assess their shape*. J. Micromech. Microeng, 2002. **12**: p. 111-114.
 56. Chae, Y.H., *Effect of size for micro-scale dimples on surface under lubricated sliding contact*, in *Mechanical Behavior of Materials X, Pts 1 and 2*, S.W. Nam, et al., Editors. 2007, Trans Tech Publications Ltd: Stafa-Zurich. p. 765-768.
 57. Zhang, J.Y. and Y.G. Meng, *A study of surface texturing of carbon steel by photochemical machining*. Journal of Materials Processing Technology, 2012. **212**(10): p. 2133-2140.
 58. Leyendecker, R. and G. Heinke, *Method and apparatus for reducing fretting wear between relatively moving parts*, in *USPTO1976*, Robert Bosch G.m.b.H: United States.
 59. Schonenberger, I. and S. Roy, *Microscale pattern transfer without photolithography of substrates*. Electrochimica Acta, 2005. **51**(5): p. 809-819.
 60. Shinkarenko, A., Y. Kligerman, and I. Etsion, *The Validity of Linear Elasticity in Analyzing Surface Texturing Effect for Elastohydrodynamic Lubrication*. Journal of Tribology-Transactions of the Asme, 2009. **131**(2).
 61. Bowden, N., et al., *Self-assembly of mesoscale objects into ordered two-dimensional arrays*. Science, 1997. **276**(11 Apr): p. 232-235.
 62. Ishibashi, K., *Methods for treating the surface of a solid body*, in *USPTO1993*: US.
 63. Srinivasarao, M., et al., *Three-dimensionally ordered array of air bubbles in a polymer film*. Science, 2001. **292**(6 April): p. 79-83.
 64. Melcher, R.L., L.T. Romankiw, and R.J. Von Gutfeld, *Method for maskless chemical machining*, in *USPTO1983*, IBM: US.
 65. Tian, H., N. Saka, and N.P. Suh, *Boundary lubrication studies on undulated titanium surfaces*. Tribology Transactions, 1989. **32**(3): p. 289-296.
 66. Li, L. and D.M. Chai, *The research and application of honing technology*. Key Engineering Materials, 2001. **202-203**: p. 385-388.
 67. Nguyen, T.A. and D.L. Butler, *Simulation of precision grinding process, part 1: generation of the grinding wheel surface*. International Journal of Machine Tools & Manufacture, 2005. **45**(11): p. 1321-1328.
 68. Tian, H. and A.M. Chao, *Optimization of disk surface texturing and lubrication on CSS performance*. IEEE Trans. Magnet., 1996. **32**(5): p. 3666-3668.
 69. Gordon, N., D. Starosvetsky, and Y. Ein-Eli, *Negative potential dissolution (NPD)-advanced and rapid texturing method of as-cut silicon*. Electrochimica Acta, 2005. **50**(27): p. 5313-5321.
 70. Cooper, C.V., P. Holiday, and A. Matthews, *The effect of tin interlayers on the indentation behavior of diamond-like carbon-films on alloy and compound substrates*. Surface & Coatings Technology, 1994. **63**(3): p. 129-134.
 71. Costa, H.L. and I.M. Hutchings, *Development of a Maskless Electrochemical Texturing Method*. Journal of Materials Processing Technology, 2009. **209**(8): p. 3869-3878.
 72. Zhu, D., et al., *Model-based virtual surface texturing for concentrated conformal-contact lubrication*. Proceedings of the Institution of Mechanical Engineers Part J-Journal of Engineering Tribology, 2010. **224**(J8): p. 685-696.
 73. Slikkerveer, P.J. and F.H. Veld, *Model for patterned erosion*. Wear, 1999. **233-235**: p. 377-386.
 74. Mastud, S., et al., *Experimental Characterization of Vibration-Assisted Reverse Micro Electrical Discharge Machining (EDM) For Surface Texturing*. Proceedings of the Asme International Manufacturing Science and Engineering Conference, 20122012. 439-448.

- 1
 - 2
 - 3
 - 4
 - 5
 - 6
 - 7
 - 8
 - 9
 - 10
 - 11
 - 12
 - 13
 - 14
 - 15
 - 16
 - 17
 - 18
 - 19
 - 20
 - 21
 - 22
 - 23
 - 24
 - 25
 - 26
 - 27
 - 28
 - 29
 - 30
 - 31
 - 32
 - 33
 - 34
 - 35
 - 36
 - 37
 - 38
 - 39
 - 40
 - 41
 - 42
 - 43
 - 44
 - 45
 - 46
 - 47
 - 48
 - 49
 - 50
 - 51
 - 52
 - 53
 - 54
 - 55
 - 56
 - 57
 - 58
 - 59
 - 60
75. Byun, J.W., et al., *Surface Texturing by Micro ECM for Friction Reduction*. International Journal of Precision Engineering and Manufacturing, 2010. **11**(5): p. 747-753.
76. Stutzmann, N., et al., *Patterning of polymer-supported metal films by microcutting*. Nature, 2000. **407**(5 October): p. 613-616.
77. Heuberger, M., et al., *Dynamic control of friction via surface structuring*, in *Boundary and Mixed Lubrication: Science and Applications*, D. Dowson, Editor 2002, Elsevier. p. 67-73.
78. Bulatov, V.P., V.A. Krasny, and Y.G. Schneider, *Basics of machining methods to yield wear- and fretting-resistive surfaces, having regular roughness patterns*. Wear, 1997. **208**: p. 132-137.
79. dos Santos, D.S., et al., *The role of azopolymer/dendrimer layer-by-layer film architecture in photoinduced birefringence and the formation of surface-relief gratings*. Langmuir, 2006. **22**(14): p. 6177-6180.
80. Okamoto, T., et al., *Ultraviolet-cured polymer microlens arrays*. Applied Optics, 1999. **38**(14): p. 2991-2996.
81. De Mello, J.D.B., J.L. Goncalves, Jr., and H.L. Costa, *Influence of surface texturing and hard chromium coating on the wear of steels used in cold rolling mill rolls*. Wear, 2013. **302**(1-2): p. 1295-1309.
82. Steinhoff, K., A. Kapoor, and N. Guillon, *Controlled wear as mechanism for the design of geometrically defined nanometric surface structures on forming tools*. Advanced Technology of Plasticity, 1999. **1**: p. 265- 270.
83. Fletcher, D.I., et al., *Wear behaviour and surface form evaluation of a novel titanium carbide implanted surface under lubricated conditions*. Proc. Inst. Mech. Engrs., 2000. **214**(J): p. 597-610.
84. Costa, H.L., et al. *Alternative methods for surface texturing*. in *1st International Brazilian Conference on Tribology*. 2010. Rio de Janeiro, Brazil: ABM.
85. Gutierrez-Mora, F., et al., *Dry and oil-lubricated sliding wear of Si₃N₄ and Si₃N₄/BN fibrous monoliths*. Tribology Letters, 2005. **18**(2): p. 231-237.
86. McGillis, D.A., *Lithography*, in *VLSI Technology*, S.M. Sze, Editor 1983, McGrawHill. p. 267-302.
87. Pardo, D.A., *Application of screen printing in the fabrication of organic light-emitting devices*. Advanced Materials, 2000. **12**(7): p. 1249-1252.
88. Vicenzi, D., *Low power thick-film gas sensor obtained by a combination of screen-printing and micromachining techniques*. Thin Solid Films, 2001. **391**: p. 288-292.
89. Leppavuori, S., et al., *A novel thick-film technique, gravure offset printing, for the realization of fine-line sensor structures*. Sensors and Actuators A, 1994. **41-42**: p. 593-596.
90. Michel, B., et al., *Printing meets lithography: soft approaches to high-resolution patterning*. IBM J. Res. & Dev., 2001. **45**(3): p. 697-719.
91. Darhuber, A.A. and S. Wagner, *Physical mechanisms governing pattern fidelity in microscale offset printing*. Journal of Applied Physics, 2001. **90**(7): p. 3602-3609.
92. Rempelbe, V.H., *Hot-stamping becomes economical for large areas*. Modern Plastics, 1970. **47**(9): p. 112-114.
93. Kumar, A.V. and A. Dutta, *Electrophotographic layered manufacturing*. Journal of Manufacturing Science and Engineering, 2004. **126**(August): p. 571-576.
94. Carlson, C.F. and J. Heights, *Electrophotography*, in *USPTO1942*.
95. Castrejon-Pita, J.R., et al., *Future, opportunities and challenges of inkjet technologies*. Atomization and Sprays, 2013. **23**(6): p. 541-565.

- 1
2
3
4
5
6
7
8
9
10
11
12
13
14
15
16
17
18
19
20
21
22
23
24
25
26
27
28
29
30
31
32
33
34
35
36
37
38
39
40
41
42
43
44
45
46
47
48
49
50
51
52
53
54
55
56
57
58
59
60
96. Costa, H.L., *Modification of surface topography: manufacturing methods and applications*, in *Engineering Department*2005, University of Cambridge: Cambridge. p. 240.
97. Marian, V.G., et al., *Theoretical and Experimental Analysis of a Laser Textured Thrust Bearing*. *Tribology letters*, 2011. **44**(3): p. 335-343.
98. Madou, M.J., *Fundamentals of Microfabrication*. 2nd ed. The Science of Miniaturization2002, Florida: CRC Press. 723.
99. Vishnitsky, A., *Electrochemical rifling of gun barrels*, in *USPTO*1987, Cation Corporation: United States.
100. Parreira, J.G., C.A. Gallo, and H.L. Costa, *New Advances on Maskless Electrochemical Texturing (MECT) for Tribological Purposes*. *Surf. Coat. Tech.*, 2012. **212**: p. 1-13.
101. James, M. *Photochemical Machining by Ink Jet. A Revolution in the Making?* in *NIP20: International Conference on Digital Printing Technologies*. 2004. Salt Lake City: IS&T.
102. Muhl, J. and G.M. Alder, *Direct Printing of Etch Masks under Computer Control*. *International Journal of Machine Tools & Manufacture*, 1995. **35**(2): p. 333-337.
103. Muhl, J., *Surface treatment of an object*, in *WIPO*1995: International Bureau.
104. Gennes, P.-G.d., F. Brochard-Wyart, and D. Quere, *Wetting of textured surfaces*, in *Capillarity and Wetting Phenomena: Drops, Bubbles, Pearls, Waves*2003, Springer. p. 216-226.
105. Vilhena, L.M., et al., *Surface texturing by pulsed Nd:YAG laser*. *Tribology International*, 2009. **42**(10): p. 1496-1504.
106. Costa, H.L. and I.M. Hutchings. *Ink-jet printing for patterning engineering surfaces*. in *NIP24/Digital fabrication 2008: 24th International conference on digital printing technologies*. 2008. Pittsburgh, PA.

List of figures

Figure 1. Schematic representation of the tree structures for methods involving: (a) removing material; (b) adding material; (c) moving material; (d) self-forming by wear.

Figure 2. Schematics of the tree structure for methods for mask generation.

Figure 3. Examples of the surface topography texture patterns generated by photochemical texturing using: (a and b) positive photoresist, circular pockets; and (c and d) negative photoresist, circular pillars; images on left show 3D maps and on right show line profiles.

Figure 4. Examples of a steel sample textured by MECT, adapted from [100], with permission: (a) 3D map of a regular array of pockets; (b) profile across a line of circular pockets; (c) 3D map of a regular array of chevrons; (d) profile across the vertices of the chevrons.

Figure 5. Contact angle measurements for different cleaning routines, average of five measurements, for magenta and black inks and water.

Figure 6. Contact angle measurements on steel samples with different surface roughness; larger grit sizes give smoother surfaces.

Figure 7. Printing of individual dots, DMP-2800 printer (adapted from [106]): (a) optical microscopy after printing; (b) 3D map after etching and stripping; (c) line profile.

1
2
3
4
5
6
7
8
9
10
11
12
13
14
15
16
17
18
19
20
21
22
23
24
25
26
27
28
29
30
31
32
33
34
35
36
37
38
39
40
41
42
43
44
45
46
47
48
49
50
51
52
53
54
55
56
57
58
59
60

Figure 8. Examples of complex shapes printed with a flatbed eagle printer and UV-curable ink: (a) parallel linear gaps; (b) rectangular gaps; (c) interrupted linear gaps; (d) chevrons, single-step printing using four printheads; (e) chevrons, multiple-step printing using one individual printhead.

Figure 9. Examples of complex printings using DMP-2800 printer, solvent-base ink; adapted from [106], with permission: (a) 20 μm gap between parallel printed lines; (b) 40 μm square gap; (c) chevrons.

Figure 10. Geometrical definitions of the textured patterns.

Figure 11. Comparison (average strokes) between film thickness for smooth and textured samples: (a) 16 mm brass cylinder, normal load = 2.5 N, samples T16 (circles) and T17 (lines); (b) 200 mm aluminium cylinder, load = 51.5N, circles, effect of area coverage (f), adapted from [4], with permission.

Figure 12. Triboscopic maps for textured (left) and smooth (right) surfaces: (a) 2.94 N, textured; (b) 2.94 N, smooth; (c) 51.94 N, smooth; (d) 51.94 N, smooth, adapted from [100], with permission.

Figure 13. SEM Of the wear tracks, BSE: (a) textured sample, 2.94N; (b) smooth sample, 12.7N.

List of tables

Table I. Experimental conditions for the photolithographic procedure.

Table II. Cleaning routines before inkjet printing; USC = ultrasonic cleaning; HAB = hot air blower; IMS = industrial methylated spirit.

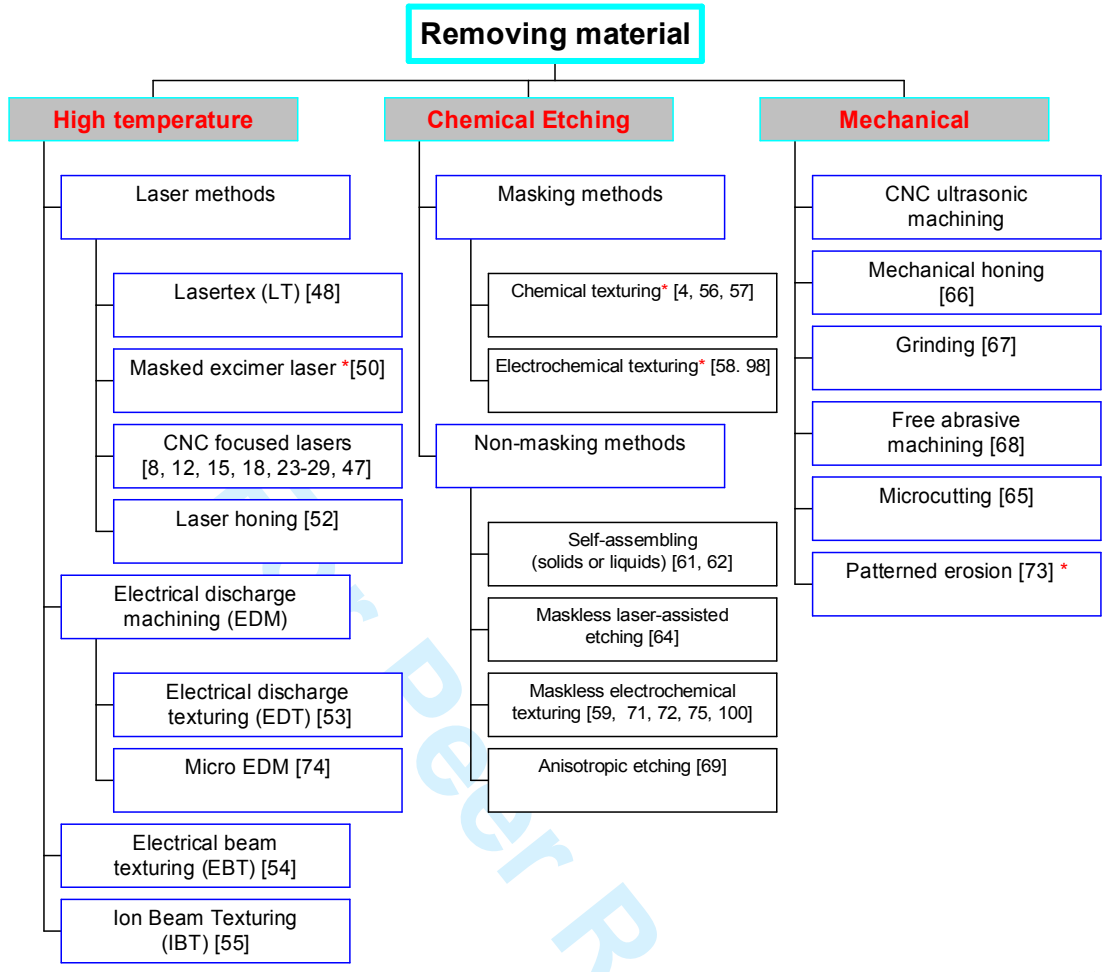
Table III. Summary of the alternative texturing methods; the geometrical dimensions of the features are defined in Figure 10.

Table IV. Dimensions (in μm) of the features in the texture patterns; NA = not applicable; the nomenclature for the dimensions is described in Figure 10.

Table V. Normal loads and corresponding contact pressures and elastic contact widths, calculated from Hertz equation.

Table VI. Normal loads with respective Hertz calculations.

1
2
3
4
5
6
7
8
9
10
11
12
13
14
15
16
17
18
19
20
21
22
23
24
25
26
27
28
29
30
31
32
33
34
35
36
37
38
39
40
41
42
43
44
45
46
47
48
49
50
51
52
53
54
55
56
57
58
59
60



(a)

Fig. 1

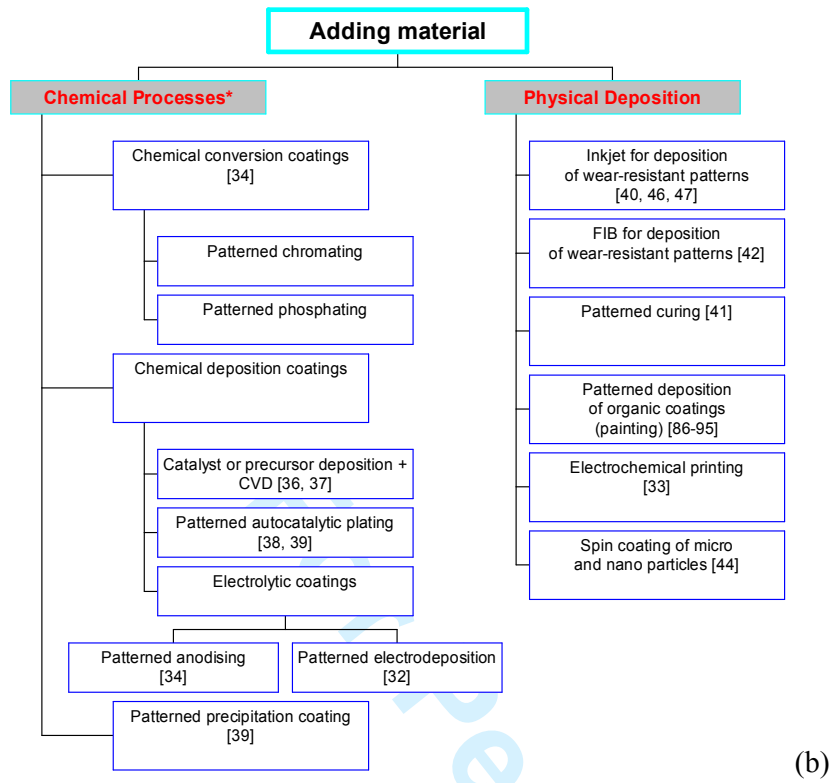
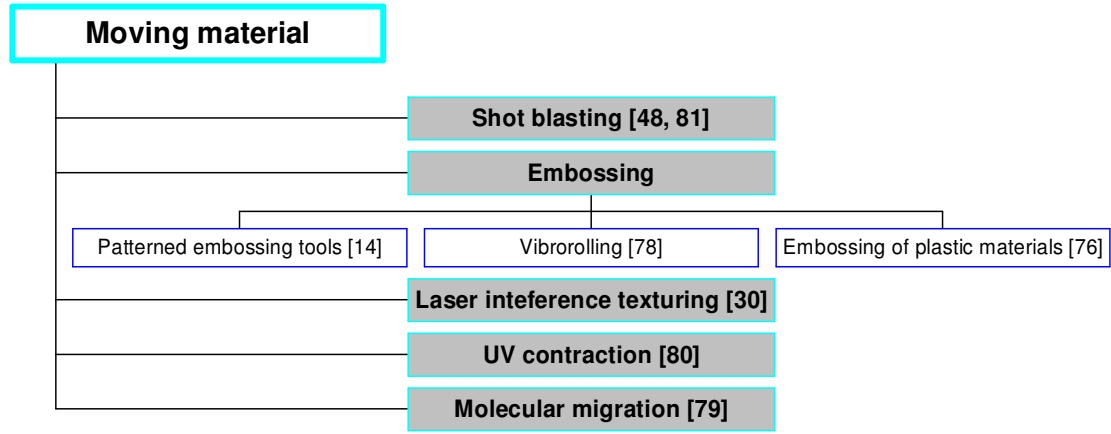


Fig. 1

1
2
3
4
5
6
7
8
9
10
11
12
13
14
15
16
17
18
19
20
21
22
23
24
25
26
27
28
29
30
31
32
33
34
35
36
37
38
39
40
41
42
43
44
45
46
47
48
49
50
51
52
53
54
55
56
57
58
59
60



(c)

Fig. 1

For Peer Review

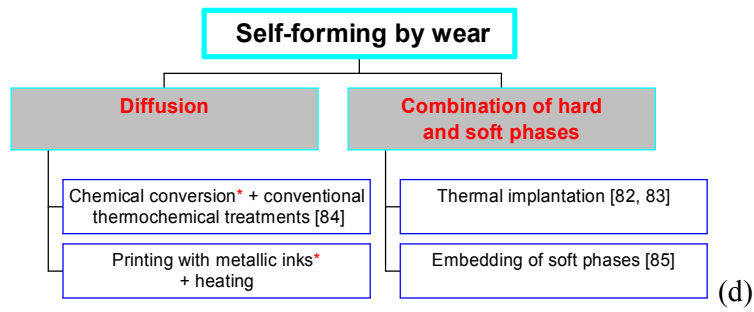


Fig. 1

For Peer Review

1
2
3
4
5
6
7
8
9
10
11
12
13
14
15
16
17
18
19
20
21
22
23
24
25
26
27
28
29
30
31
32
33
34
35
36
37
38
39
40
41
42
43
44
45
46
47
48
49
50
51
52
53
54
55
56
57
58
59
60

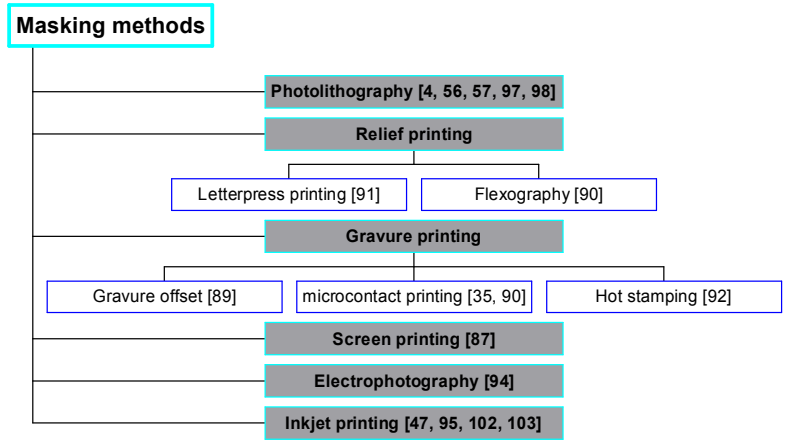
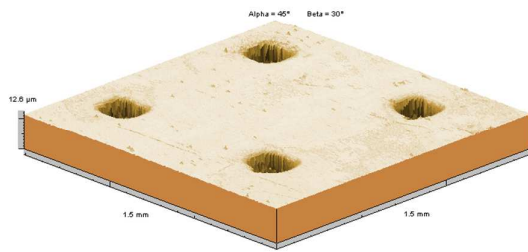


Fig. 2

For Peer Review

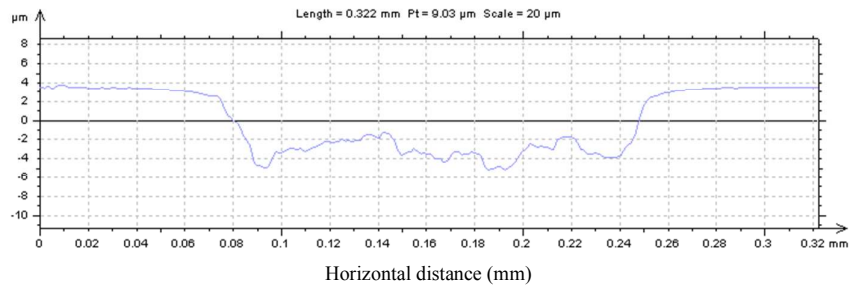


(a)

Figure 3

For Peer Review

1
2
3
4
5
6
7
8
9
10
11
12
13
14
15
16
17
18
19
20
21
22
23
24
25
26
27
28
29
30
31
32
33
34
35
36
37
38
39
40
41
42
43
44
45
46
47
48
49
50
51
52
53
54
55
56
57
58
59
60



(b)

Figure 3

For Peer Review

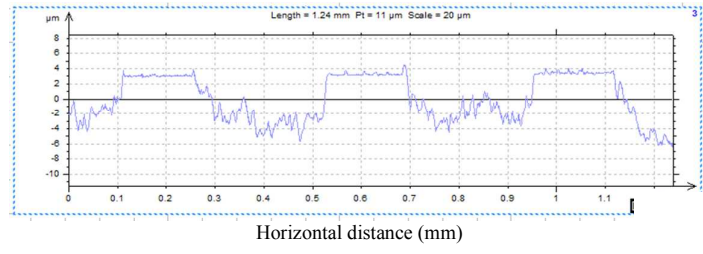


(c)

Figure 3

For Peer Review

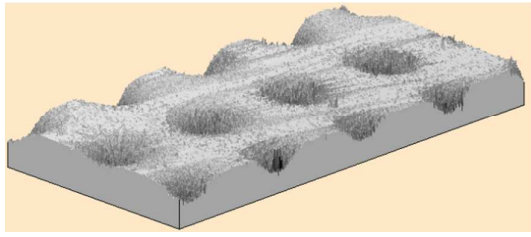
1
2
3
4
5
6
7
8
9
10
11
12
13
14
15
16
17
18
19
20
21
22
23
24
25
26
27
28
29
30
31
32
33
34
35
36
37
38
39
40
41
42
43
44
45
46
47
48
49
50
51
52
53
54
55
56
57
58
59
60



(d)

Figure 3

For Peer Review

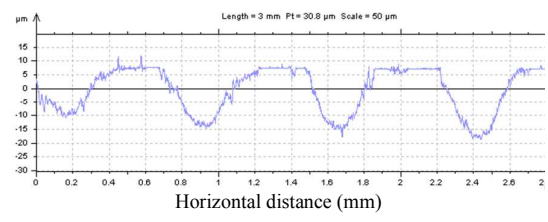


(a)

Figure 4

For Peer Review

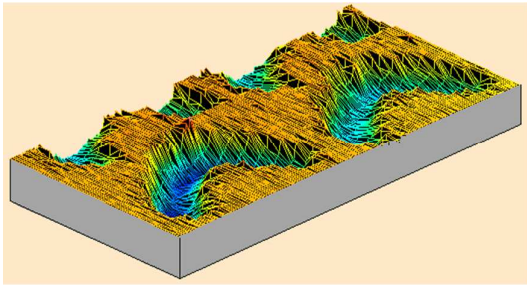
1
2
3
4
5
6
7
8
9
10
11
12
13
14
15
16
17
18
19
20
21
22
23
24
25
26
27
28
29
30
31
32
33
34
35
36
37
38
39
40
41
42
43
44
45
46
47
48
49
50
51
52
53
54
55
56
57
58
59
60



(b)

Figure 4

For Peer Review

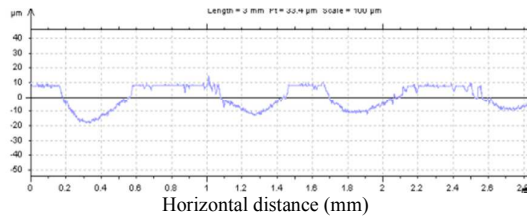


(c)

Figure 4

For Peer Review

1
2
3
4
5
6
7
8
9
10
11
12
13
14
15
16
17
18
19
20
21
22
23
24
25
26
27
28
29
30
31
32
33
34
35
36
37
38
39
40
41
42
43
44
45
46
47
48
49
50
51
52
53
54
55
56
57
58
59
60



(d)

Figure 4

For Peer Review

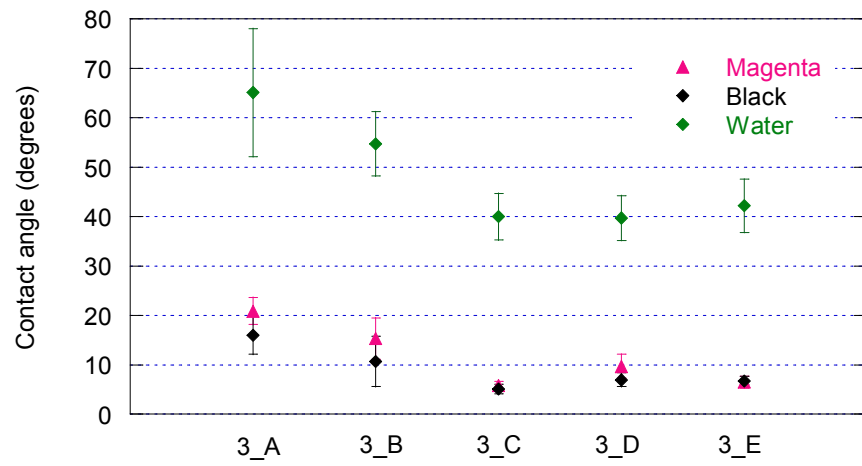


Figure 5

1
2
3
4
5
6
7
8
9
10
11
12
13
14
15
16
17
18
19
20
21
22
23
24
25
26
27
28
29
30
31
32
33
34
35
36
37
38
39
40
41
42
43
44
45
46
47
48
49
50
51
52
53
54
55
56
57
58
59
60

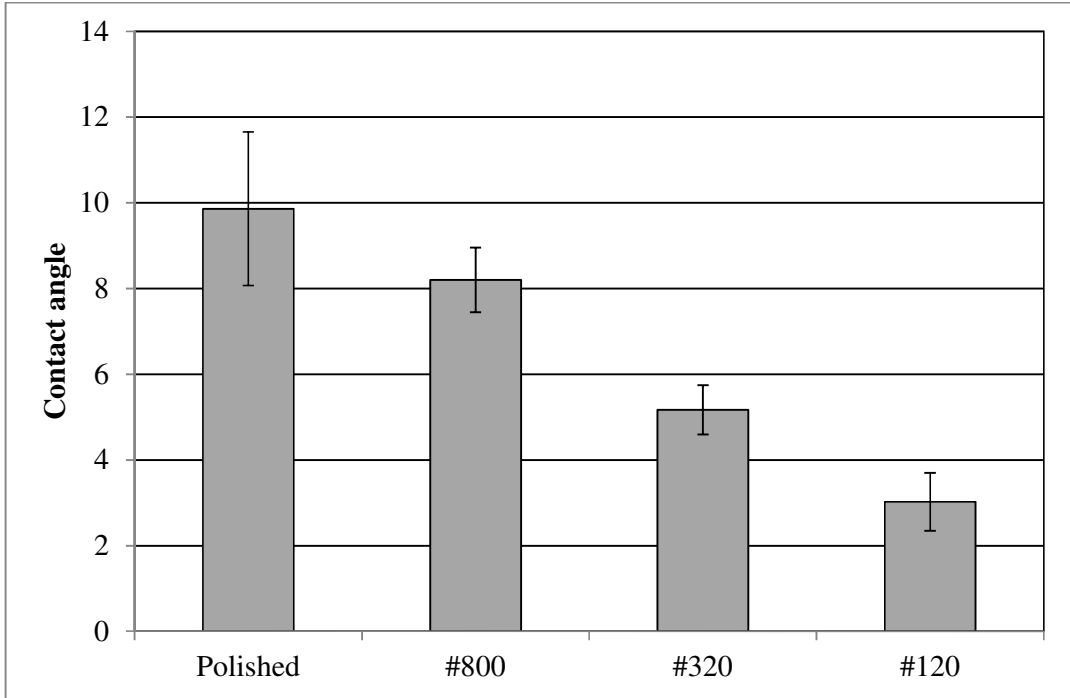
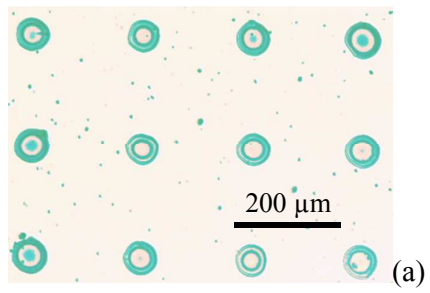


Figure 6

Peer Review



15 Figure 7

16
17
18
19
20
21
22
23
24
25
26
27
28
29
30
31
32
33
34
35
36
37
38
39
40
41
42
43
44
45
46
47
48
49
50
51
52
53
54
55
56
57
58
59
60

For Peer Review

1
2
3
4
5
6
7
8
9
10
11
12
13
14
15
16
17
18
19
20
21
22
23
24
25
26
27
28
29
30
31
32
33
34
35
36
37
38
39
40
41
42
43
44
45
46
47
48
49
50
51
52
53
54
55
56
57
58
59
60

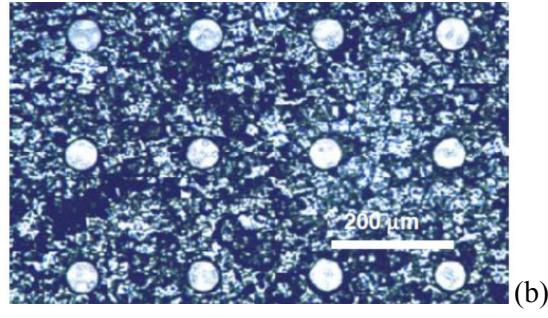
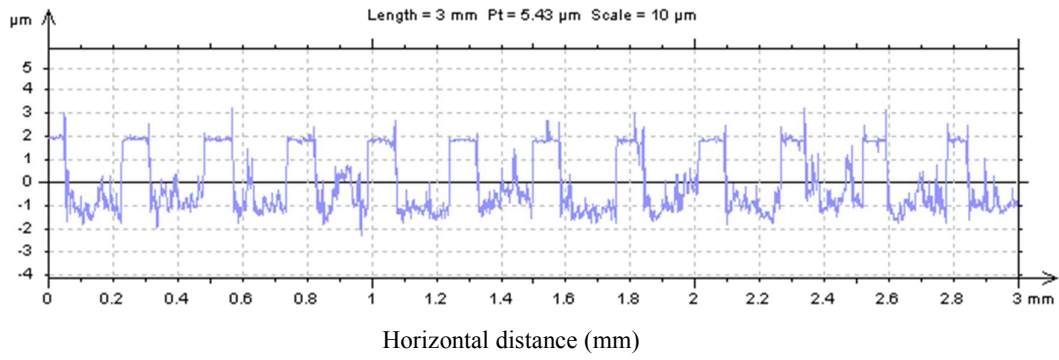


Figure 7

For Peer Review



(c)

Figure 7

For Peer Review

1
2
3
4
5
6
7
8
9
10
11
12
13
14
15
16
17
18
19
20
21
22
23
24
25
26
27
28
29
30
31
32
33
34
35
36
37
38
39
40
41
42
43
44
45
46
47
48
49
50
51
52
53
54
55
56
57
58
59
60

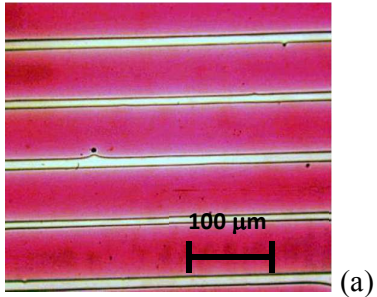
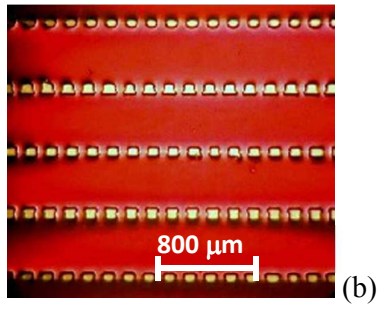


Figure 8

For Peer Review

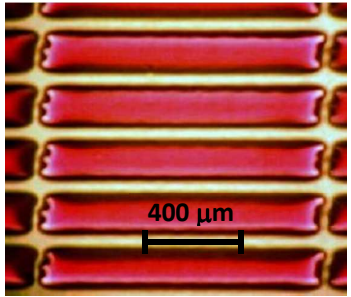


15
16
17
18
19
20
21
22
23
24
25
26
27
28
29
30
31
32
33
34
35
36
37
38
39
40
41
42
43
44
45
46
47
48
49
50
51
52
53
54
55
56
57
58
59
60

Figure 8

For Peer Review

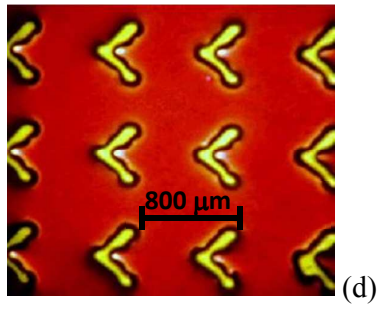
1
2
3
4
5
6
7
8
9
10
11
12
13
14
15
16
17
18
19
20
21
22
23
24
25
26
27
28
29
30
31
32
33
34
35
36
37
38
39
40
41
42
43
44
45
46
47
48
49
50
51
52
53
54
55
56
57
58
59
60



(c)

Figure 8

For Peer Review



15
16
17
18
19
20
21
22
23
24
25
26
27
28
29
30
31
32
33
34
35
36
37
38
39
40
41
42
43
44
45
46
47
48
49
50
51
52
53
54
55
56
57
58
59
60

Figure 8

For Peer Review

1
2
3
4
5
6
7
8
9
10
11
12
13
14
15
16
17
18
19
20
21
22
23
24
25
26
27
28
29
30
31
32
33
34
35
36
37
38
39
40
41
42
43
44
45
46
47
48
49
50
51
52
53
54
55
56
57
58
59
60

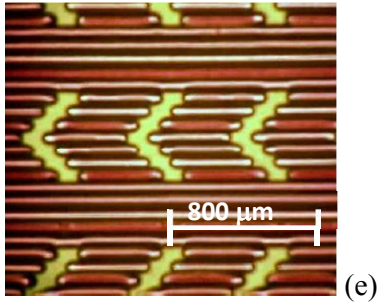
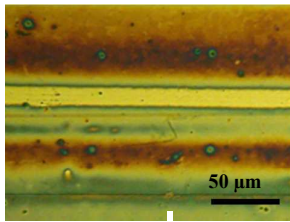


Figure 8

For Peer Review



(a)

Figure 9

For Peer Review

1
2
3
4
5
6
7
8
9
10
11
12
13
14
15
16
17
18
19
20
21
22
23
24
25
26
27
28
29
30
31
32
33
34
35
36
37
38
39
40
41
42
43
44
45
46
47
48
49
50
51
52
53
54
55
56
57
58
59
60

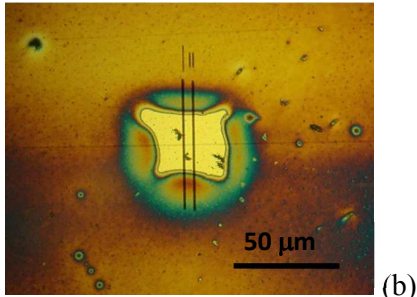


Figure 9

For Peer Review

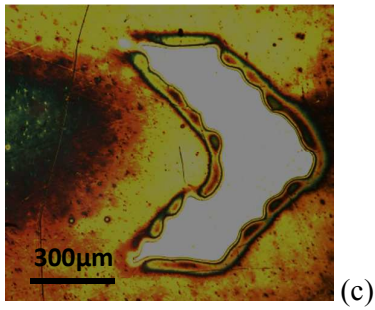


Figure 9

For Peer Review

1
2
3
4
5
6
7
8
9
10
11
12
13
14
15
16
17
18
19
20
21
22
23
24
25
26
27
28
29
30
31
32
33
34
35
36
37
38
39
40
41
42
43
44
45
46
47
48
49
50
51
52
53
54
55
56
57
58
59
60

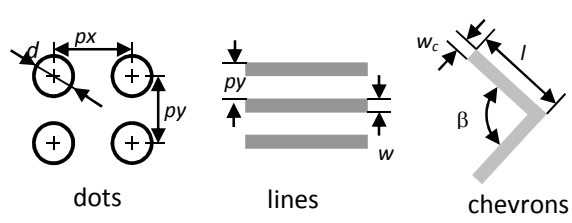


Figure 10

For Peer Review

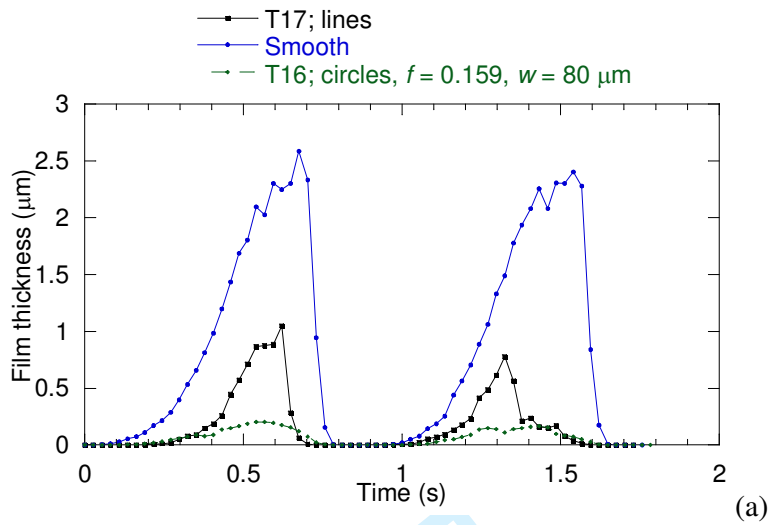
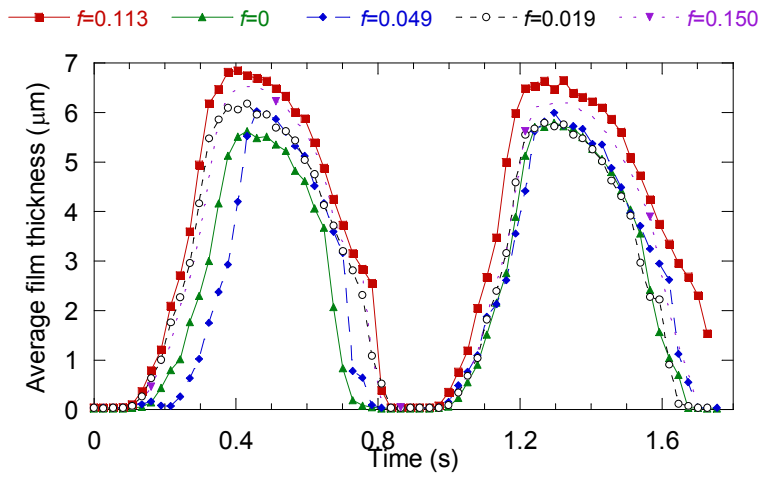


Figure 11



(b)

Figure 11

Peer Review

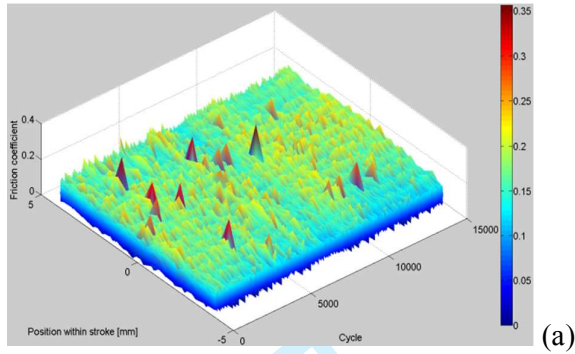


Figure 12

For Peer Review

1
2
3
4
5
6
7
8
9
10
11
12
13
14
15
16
17
18
19
20
21
22
23
24
25
26
27
28
29
30
31
32
33
34
35
36
37
38
39
40
41
42
43
44
45
46
47
48
49
50
51
52
53
54
55
56
57
58
59
60

1
2
3
4
5
6
7
8
9
10
11
12
13
14
15
16
17
18
19
20
21
22
23
24
25
26
27
28
29
30
31
32
33
34
35
36
37
38
39
40
41
42
43
44
45
46
47
48
49
50
51
52
53
54
55
56
57
58
59
60

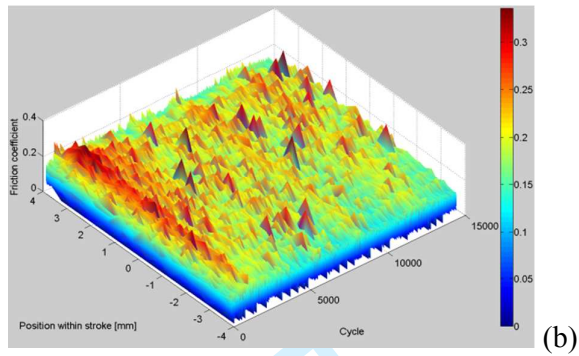


Figure 12

For Peer Review

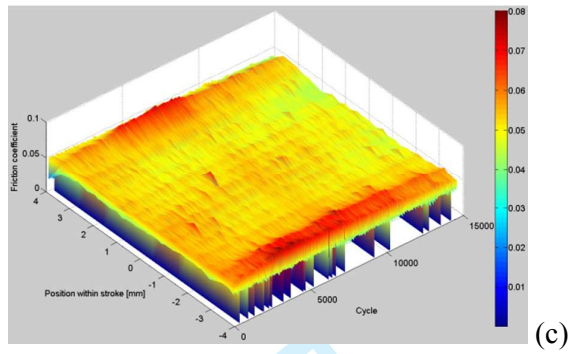


Figure 12

1
2
3
4
5
6
7
8
9
10
11
12
13
14
15
16
17
18
19
20
21
22
23
24
25
26
27
28
29
30
31
32
33
34
35
36
37
38
39
40
41
42
43
44
45
46
47
48
49
50
51
52
53
54
55
56
57
58
59
60

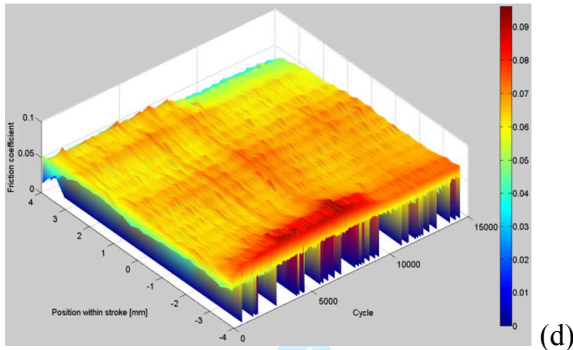
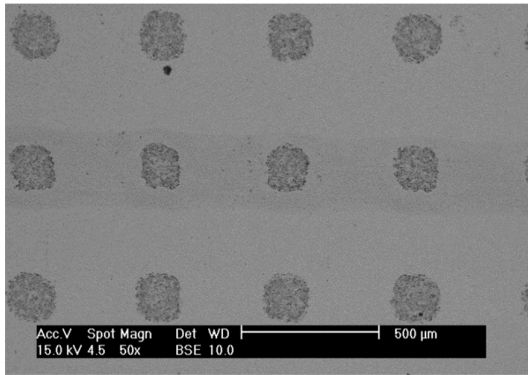


Figure 12

For Peer Review



(a)

Figure 13

Or Peer Review

1
2
3
4
5
6
7
8
9
10
11
12
13
14
15
16
17
18
19
20
21
22
23
24
25
26
27
28
29
30
31
32
33
34
35
36
37
38
39
40
41
42
43
44
45
46
47
48
49
50
51
52
53
54
55
56
57
58
59
60

1
2
3
4
5
6
7
8
9
10
11
12
13
14
15
16
17
18
19
20
21
22
23
24
25
26
27
28
29
30
31
32
33
34
35
36
37
38
39
40
41
42
43
44
45
46
47
48
49
50
51
52
53
54
55
56
57
58
59
60

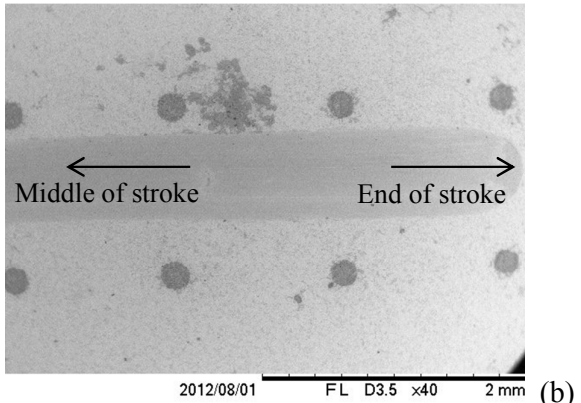


Figure 13

Or Peer Review

Table I

Conditions	Negative resist	Positive resist
Spinning rotation (rpm)	3000	4000
Spinning time (s)	60	30
Pre-baking temperature (°C)	95	95
Pre-baking time (s)	60	60
Exposure time (s)	300	300
Developing time (s)	180	30-60
Post-baking temperature (°C)	150	150
Post-baking time (s)	180	180

For Peer Review

Table II

Sample	SURFACE CONDITIONS
3_A	Polished (1 μm diamond) one month before and cleaned with acetone
3_B	Polished (1 μm diamond) up to 4 h before and cleaned with acetone
3_C	Condition 3_B, cleaned for 5 min. in 36%wt NaCO_3 using USC, rinsed, sprayed with IMS and dried with HAB
3_D	Condition 3_B, cleaned for 5 min. in 36%wt NaCO_3 using USC, rinsed, cleaned for 5 min. in detergent + warm water, rinsed, sprayed with IMS and dried with HAB
3_E	Condition 3_A, cleaned cleaned for 5 min. in 36%wt NaCO_3 using USC, rinsed, sprayed with IMS and dried with HAB

For Peer Review

Table III

	Characteristic	LT		MECT	PCT*	Inkjet printing
		ns	fs			
Geometric resolution	d (μm)	10	< 5	150	20	40
	h (μm)	3	<1	5	2	3
	w (μm)	10	<5	200	20	20
	w_c (μm)	10	<5	400	40	150
Possible substrate curvatures	Flat	Yes	Yes	Yes	Yes	Yes
	Low curvature	Yes	Yes	With adaptation	Yes	No
	Cylindrical	Yes	Yes	With adaptation	Yes	No
Cost	Commercially available	Yes	Yes	No	No	Yes
	Capital cost***	++++	+++++	+	++	+++
	Texturing cost***	+++	+++	+	++	+++
	Texturing time**	20-45 min	30 s-5min	30s	15 min	8-10 min
Possible substrate materials	Metals	Yes	Yes	Yes	Yes	Yes
	Ceramics	Yes	Yes	Some	Yes	Yes
	Polymers	Yes	Yes	No	No	No

*the characteristics presented are based on the simplified version presented in this paper and not using conventional photolithography.

**approximate time for texturing a smooth clean area of 100 x 100 mm, $d = 150 \mu\text{m}$, $h = 20 \mu\text{m}$, $f = 0.15$, no pre or post-treatment included.

*** “+” means very low and “+++++” means high.

1
2
3
4
5
6
7
8
9
10
11
12
13
14
15
16
17
18
19
20
21
22
23
24
25
26
27
28
29
30
31
32
33
34
35
36
37
38
39
40
41
42
43
44
45
46
47
48
49
50
51
52
53
54
55
56
57
58
59
60

Table IV

Pattern	Sample	<i>h</i>	<i>d</i>	<i>Px or Py</i>	<i>w</i>	β	<i>l</i>
Circles	T1	4.5	41		NA	NA	NA
	T2	4.5	40		NA	NA	NA
	T3	4.5	47		NA	NA	NA
	T4	6	70		NA	NA	NA
	T16	2	80	56	NA	NA	NA
Lines	T17	4.5	NA	52	42	NA	NA
Chevrons	T10	4.5	NA	NA	132	70	190

Table V

Load (N)	16 mm brass cylinder		200 mm aluminum cylinder	
	Contact width (μm)	Contact pressure (MPa)	Contact width (μm)	Contact pressure (MPa)
2.5	9.2	472	Not used	
12.3	21	2320	82	146
22.1	Not used		111	262
31.9			133	379
41.7			152	496
51.5			169	612
61.3			184	729
71.1			198	845
80.9			212	962

1
2
3
4
5
6
7
8
9
10
11
12
13
14
15
16
17
18
19
20
21
22
23
24
25
26
27
28
29
30
31
32
33
34
35
36
37
38
39
40
41
42
43
44
45
46
47
48
49
50
51
52
53
54
55
56
57
58
59
60

Table VI

Normal load (N)	Maximum contact pressure (MPa)	Contact width CW (μm)	d/CW
2.94	631	94.4	2.1
12.74	1029	153.8	1.2
51.94	1643	245.7	0.8

For Peer Review